# WARPING STRESSES AND DEFLECTIONS IN CONCRETE SLABS

MAY 1958
NO. 12



Joint Highway Research Project

PURDUE UNIVERSITY
LAFAYETTE INDIANA

by

M. E. HARR

FINAL REPORT

WARPING STRESSES AND DEFLECTIONS IN CONCRETE SLABS

TO: K. B. Woods, Director
Joint Highway Research Project

May 21, 1958

FROM: H. L. Michael, Assistant Director

File: 9-7-2
Project: C-36-63B

Attached is a report entitled, "Warping Stresses and Deflections in Concrete Slabs," by Mr. M. E. Harr, Research Assistant, on our staff. The project was performed under the direction of Prof. G. A. Leonards and is a continuation of the pavement deflection research which has been in progress for the past several years.

The report was also used by Mr. Harr as his thesis in partial fulfillment of the requirements for the Ph. D. degree. The author plans to prepare a technical paper from this report for submission to the Highway Research Board in 1959.

The report is presented for the record.

Respectfully submitted,

Harold L. Michael

Harold L. Michael, Assistant Director
Joint Highway Research Project

HLM:acc

Attachment

cc: A. K. Branham
J. R. Cooper
W. L. Dolch
W. H. Goetz
J. T. Hallett
F. F. Havey
G. A. Hawkins
G. A. Leonards
J. F. McLaughlin
R. D. Miles
R. E. Mills
B. H. Petty
M. B. Scott
C. E. Vogelgesang
J. L. Waling
J. E. Wilson
E. J. Yoder

FINAL REPORT

# WARPING STRESSES AND DEFLECTIONS IN CONCRETE SLABS

by

M. E. Harr, Research Assistant

Joint Highway Research Project
Project No: C-36-63B
File No: 9-7-2

Purdue University
Lafayette, Indiana

May 21, 1958

## ACKNOWLEDGMENTS

The writer wishes to express his gratitude to the Joint Highway Research Project at Purdue University, Professor K. B. Woods, Director, who sponsored this study. He is deeply appreciative of the inspiration and assistance of his major professor, Dr. G. A. Leonards, who guided the course of this work.

The author wishes to express appreciation to the Statistical and Computing Laboratory of Purdue University, with particular thanks to Mr. R. R. Partlow who programmed the problem and gave unselfishly of his time. Thanks are also due to Dr. A. C. Eringen of the Division of Engineering Sciences, Purdue University, for his helpful suggestions, and to the Portland Cement Association Laboratories, Skokie, Illinois, for making available to the author their experimental deflection data.

# TABLE OF CONTENTS

Page

# LIST OF TABLES

# LIST OF FIGURES

Page

# ABSTRACT

Harr, Milton Edward. Ph. D., Purdue University, June 1958. "Warping Stresses and Deflections in Concrete Slabs." Major Professor: G. A. Leonards.

A theory has been developed whereby the stresses, deflections, and degree of support of concrete slabs on ground, subject to ambient temperature and moisture gradients, can be computed for finite slab sizes.

Solutions to the resulting equations were programmed for the Datatron 204 digital computer at Purdue University. As a part of the solution, subroutines were developed for the Ber and Bei functions and their first derivatives.

Nomographs are presented which give ratios of the critical stress to the modulus of rupture for a wide range of environmental gradients, and for various combinations of slab sizes and thicknesses. For slab sizes and equivalent temperature gradients that comply with Westergaard's assumptions of a fully supported slab, computed stresses and deflections check those obtained by the Westergaard theory. However, the maximum gradients for which the Westergaard theory was found to be applicable are very much lower than those commonly encountered in practice. The new theory is capable of accounting for the more critical conditions, which develop when the slab is only partially supported.

Conclusive evidence regarding the reliability of the derived theory is not available at this time. However, comparisons between computed deflections and available measured deflections strongly indicate that the theory is applicable to concrete highway pavements not subject to superimposed traffic loads.

Although many factors, such as aggregates, water-cement ratios, curing, carbonation, etc., affect the moisture content-volume change relationship, the available data indicate that combined temperature and moisture gradients encountered in practice are capable of producing tensile stresses which exceed the modulus of rupture of concrete. In the critical shrinkage range, a moisture gradient of one percent can cause warping equivalent to a 20 degree F. difference in temperature between slab surfaces. Accordingly, cracking may occur at small temperature gradients if moisture differences between slab surfaces are only a few percent.

The concepts developed in this study can provide the basis for the solution of a number of problems involving warping of slabs; for example, "slab on ground" construction for homes, icing of lakes, and the like.

# INTRODUCTION

As of the end of the 1955 calendar year, approximately 100,000 miles of Portland cement concrete highways were in use in the United States. In 1955, alone, almost 2100 miles of this type of surface were constructed (46)*. According to F. B. Farrel and H. R. Patrick (9), expenditures for all types of surfacing on primary and secondary roads have comprised about 40 percent of the construction funds for highways as compared to about 25 percent, each, for grading and structures. These percentages are based on an estimate of total construction expenditures from 1914 to 1952 in relation to prevailing prices of January 1, 1953.

The average expected service life to zero salvage for concrete pavements has decreased from 27 years in 1914 to 25 years in 1953; whereas, the service life of concrete highway structures has increased from 40 years to 52 years in the same period (46,9). In addition, a great number of concrete pavements are resurfaced each year in an attempt to halt deterioration and to restore their life. The life of resurfacing is itself rather limited by "reflection cracks" from the resurfaced slab (4, 33). Usually, such cracks appear in the resurfacing during the first few years of service. According to Bone, Crump, and Roggeveen (4), "Reflection cracking is a serious problem where

---

* Figures in parentheses refer to references in the Bibliography.

bituminous resurfacings are placed over old cement-concrete pavements. The cracks detract from the appearance and riding qualities of the surface and may be expected to shorten the effective life of the resurfacing . . . there is no sure method of eliminating reflection cracking." The initial occurrence of pavement cracks is injurious not primarily from the standpoint of driving comfort as pointed out by Cashell and Teske ( 8 ), but rather from the danger of water penetration with subsequent pumping, loss of subgrade support and increased pavement deterioration (54 ). That cracks are the result of excessive tensile stresses in the concrete is well-known. However, the causes of these excessive stresses have not been properly evaluated, for obviously less than optimum performance has been obtained from concrete pavements and the remedial measures designed for them.

In the past, deterioration of unsound concrete was a primary cause of pavement failures; however, these difficiencies have been largely eliminated. According to Friberg (11 ), sound air entrained concrete is equal to well over 50-years service in climates common to the United States. Unsound aggregates have been largely eliminated. Frost-heaving on concrete roads has been greatly reduced. To be sure, unsatisfactory materials have been the cause of some pavement replacements, but they appear to be of a localized nature. As reported by W. van Breeman ( 6 ), "Almost all of the failures that have occurred with concrete pavements in New Jersey have been of a structural nature, as differentiated from failures attributable to weakness or disintegration of the concrete itself." This conclusion has also been shown in many

other investigations ( 1, 50, 8, 17, 41, 16 ). The realization of a longer service life, therefore, is not blocked by material limitations. It should be noted that even material failures seem to be peculiarily oriented near transverse cracks and joints (1,50). This is due primarily to the increased exposure of the concrete along these joints and cracks.

In recent years, application of soil mechanics principles to pavement design has largely eliminated poor subgrade support as a primary cause of concrete pavement failures. Frost susceptible soils have been isolated and effective remedial measures have become common practice ( 4, 26, 33, 53, 52, 51, 20, 17, 7 ). According to Friberg (11), "Poor subgrades cannot be disregarded as a continuing deteriorating influence. But, with the exception of localized frost heaves or unusual disturbance of soil equilibrium, subgrade instability appears to be serious exclusively at joints and cracks. Even subgrade pumping, a major sign of deterioration of the pavement, has not been of consequence away from joints [edges] and cracks."

The most common critical conditions in concrete pavements are reflected by the cracks in existing roads. The occurrence of corner or diagonal cracks, transverse cracks, and longitudinal cracks have been recorded in many published surveys of concrete pavements (1, 50, 26, 39, 2, 25, 32, 30 ). In 1952, a crack survey was made under controlled conditions on the Maryland Test Road (17). The data show a predominance of transverse cracks. As a matter of fact, recent performance surveys show that it is rather unusual to find corner failures, in modern concrete pavements, of the type analyzed by Westergaard (47), Teller and Sutherland (41), Spangler (36), and others.

On 900 miles of Louisiana 6-inch thickened pavement with 42 feet average joint spacing, Friberg (11) reports 86 percent of all cracks were transverse. Corner cracks averaged less than one per mile. On the Maryland Test Road (17), sections 1, 2, and 3, 98 percent of the cracks were transverse cracks. In 1948, H. Allen and F. H. Jackson reported on a survey of the concrete pavement on the German autobahn (20), "Transverse cracking was common and was not confined to any particular part of the system. There seemed to be no relation between transverse cracking, terrain or soil conditions." Similar data for continuously reinforced concrete pavements have also been reported ( 8 ).

Longitudinal center cracks, common in pavements prior to 1925, have been almost completely eliminated by center joint construction. However, as noted by Friberg (11), "Longitudinal cracks near the outside pavement edge, extending for a short distance from transverse joints, sometimes referred to as "infiltration cracks", appear to be increasingly common . . . on Road Test One-MD, section 4 on pumping soil, subjected to heavy tandem-axle loading, a different type of longitudinal cracking occurred. Here 11 percent of the cracks were longitudinal and all originated at transverse joints 4 to 5 feet from the edge, and extended progressively further away, finally meeting at mid-length of the 40 ft. slabs. This longitudinal cracking is an indication of critical transverse load stresses near transverse joints in connection with loss of subgrade support."

The results of many investigations have shown that the critical stresses in a concrete pavement slab, which are mirrored by structural cracks of specific orientation, are primarily due to the combined

effects of traffic loads, pavement warping, and pavement pumping (20, 11, 10, 17, 41, 48 ). To use concrete pavements with maximum economy and efficiency, it is necessary to predict, as accurately as possible, the character and magnitude of the stresses induced in a slab by continually changing environment and by the traffic loads to which it is subsequently subjected.

Concrete expands or contracts as its temperature and moisture content increases or decreases. Concrete pavements are exposed to the elements and, consequently, are subject to diurnal and seasonal changes in length. In addition, temperature and moisture differences between the tops and bottoms of slabs result in their tendency to warp.

In the past, investigators have examined the effect of the position and magnitude of the wheel loads on a pavement slab (47,36), of the presence of one wheel load near to another (37), of impact ( 5 ), and of traffic frequency (38,31). All of these analyses have been based on the assumption that the slab maintains contact with its support at all points and at all times. Recent experimental studies (12), have clearly demonstrated that this assumption may be seriously in error. Accordingly, improved analytical procedures are predicated on the development of a theory that allows for the possibility that warping may result in the slab's being only partially supported when it receives traffic loads.

It is the object of this thesis to obtain by analytical means the deflections, stresses, and degree of support of concrete slabs subject to environmental temperature and moisture gradients.

# REVIEW OF LITERATURE

## Part I

## Warping of Concrete Pavements

In 1879, Bauschinger ( 3 ) pioneered investigations into the volume changes of Portland cement concrete induced by variations of temperature and moisture. Following Bauschinger, many investigators have measured the effect of a number of factors on volume changes in concrete, among which are the effects of age of specimen, quality of cement, kind of aggregate, richness of mix, duration of exposure, and the like. An excellent discussion and bibliography of these early investigations is given by Hatt (14).

With the advent of concrete pavements, highway engineers soon became aware of the detrimental effects of volume changes. As early as 1910, the Office of Public Roads (13) conducted a series of laboratory and field tests to study the expansion and contraction of concrete pavements. In 1922, tests conducted on the Bates Experimental Road (29) led to the discovery that temperature differences between pavement surfaces result in considerable warping of the slab. As pointed out by Teller and Sutherland (41), "The early investigations were of value, first, for the information that they developed, and second, because each one served to arouse more wide-spread interest in the subject among highway engineers."

In 1925, Hatt (14) reported warping could be induced by a corresponding moisture difference between the surfaces of the slab. Hatt's studies are of special interest since they apparently represent

the only published data on the effects of moisture on concrete slabs under controlled conditions. Hatt's observations were based on studies of a concrete slab, 7 inches thick, 18 feet wide, and 25 feet long (with a longitudinal doweled center joint) on a 4-inch coarse gravel base. The slab was covered and housed to control the distribution of moisture and temperature. Among Hatt's conclusions is the following:

> Concrete road slabs warp upward at the corners and at the edges when the surface becomes dry, and also when the bottom absorbs moisture from the subgrade. Drying the top surface of the slab under observation deflected the corners upward 0.02 inches. When the bottom of the slab was saturated from a water filled subgrade the upward corner deflection reached 0.20 inches. This curling upward of the corners of the road slab presents a cantilever beam to the load of a passing truck. The results of the tests indicate the presence of an initial stress in the surface of the road slab arising from the warping.

Hatt recognized that portions of the slab could be unsupported. In fact, in reference to some load tests, he states, "As the warping of the slab increased, the point of support must have moved in, increasing the deflection." Figure 1 is reproduced from Hatt's paper. The curves clearly illustrate the degree of unsupport and the influence of moisture. It should also be noted that the maximum downward deflection does not occur at the center of the slab. All measurements of surface deformations of the slab were the result of moisture differences alone since observations were taken at times when the temperatures were constant throughout the slab.

Beginning in 1930 and continuing to their final report in 1943, the Public Road Administration, under the direction of L. W. Teller and E. C. Sutherland (41), conducted several extensive investigations to

EFFECT OF NON-UNIFORM MOISTURE
ON DEFLECTION OF TEST SLAB
AFTER : HATT (14)

FIGURE 1

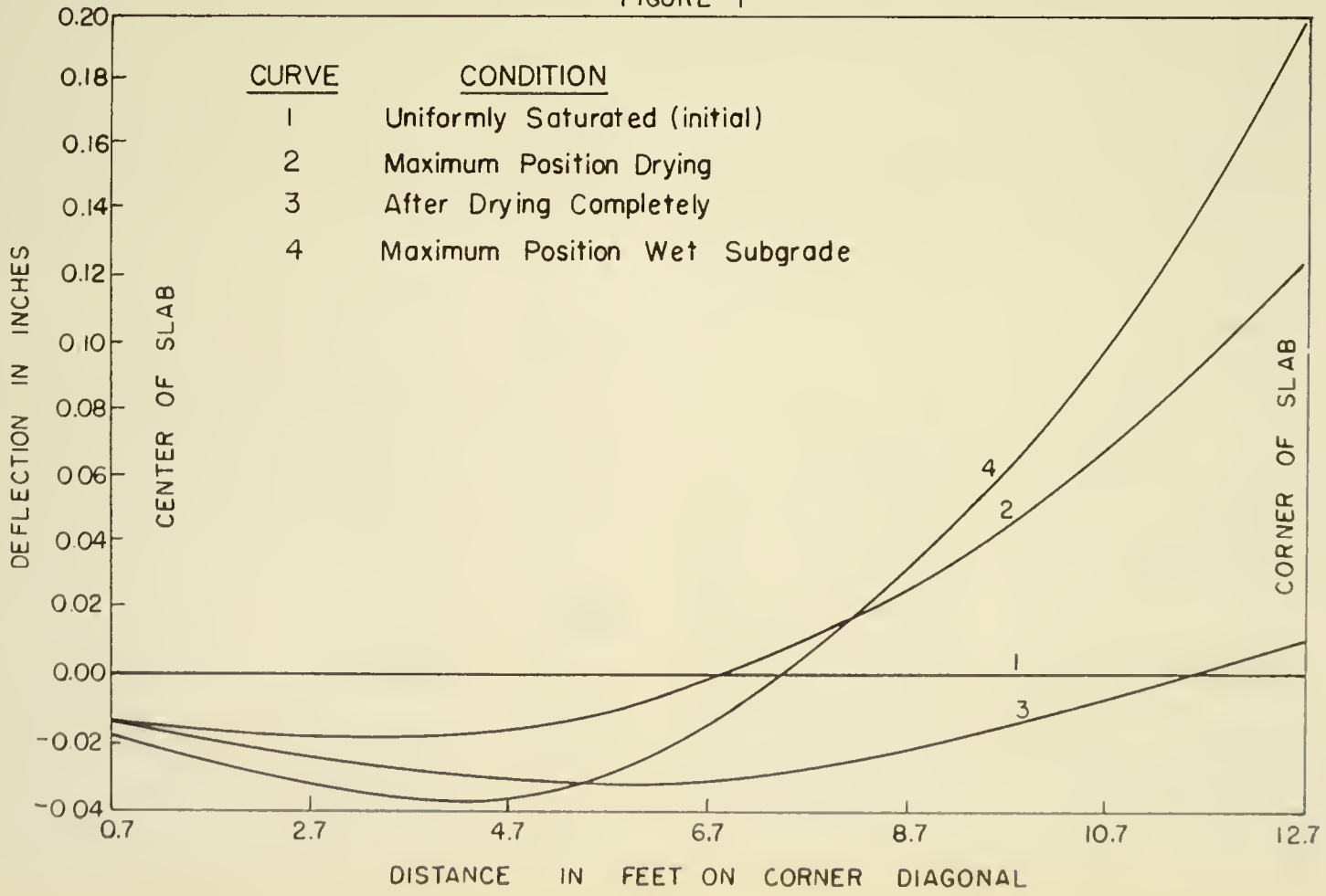

develop a better understanding of the structural action of concrete pavement slabs. The significant observations and conclusions pertinent to the present study are as follows:

1) Warping has two important effects on the structural action of a pavement slab. In the first place, the distortion that occurs alters the conditions of subgrade support and thus affects the magnitude of the stress that will be produced by a given wheel load. In the second place, because of the weight of the slab, the warping in itself causes important stresses within the slab structure. Both of these actions place limitations on the maximum wheel load that may be carried by the pavement, and, for this reason, any information concerning them is of value.

2) In the early morning and in the afternoon when the maximum temperature differentials occur, there is approximately a straight-line gradient in temperature between upper and lower surfaces of the concrete. These are the two times of the day that are most important in the determination of stress caused by warping. [Due to the lack of instrumentation it was not possible to determine moisture gradients. Figure 28 of the report indicates that there was relatively little difference in upward deflection between the free edge and the longitudinal joint, and the free end and the transverse joint.]

3) A comparison of the relative magnitudes of the stresses created by warping at the center of the slab [10 x 20 feet] in the transverse and longitudinal directions shows that the stress in the direction of the 10 foot dimension is approximately one-third of that in the 20 foot dimension.

4) The actual temperature differential between upper and lower surfaces of the slab is always greater for the thicker slab. [The maximum positive temperature gradient (bottom temperature greater than top) at the test site (Arlington, Virginia) was approximately 1-1/2 degrees per inch. No information as to moisture gradients was noted.]

In summarizing their data, the authors state:

> The data that have just been presented clearly indicate that the stresses arising from restrained temperature warping equal in importance those caused by the heaviest wheel loads. The stresses from this cause are actually large enough to cause failure in concrete of low flexural strength, and since the direction of the stresses is such that they become added to the critical stresses caused by wheel loads, there is little doubt but that warping stress is primarily responsible for much of the cracking in concrete pavements.

More recent tests (1952), conducted in southern Maryland as a part of "Road Test One-MD" (17), indicate that for corner loading the stresses and deflections for severe downward-warped conditions are only approximately one-third those for the critical upward-warped conditions. For the free-edge loading the effect of temperature warping, although appreciable, was not as pronounced as for the case of the corner loading.

In 1944, the California Division of Highways, reflecting the concern of highway engineers throughout the United States, began extensive field and laboratory studies to determine the cause of distress at the joints of concrete pavements. The results of this study were reported by F. N. Hveem (18). Hveem's comments on subgrade support follows:

> Engineers have paid much attention to subgrade support for concrete pavements at or near the planned joints in the pavement, but if it is recognized that for a considerable portion of time rigid pavements do not rest on the subgrade for several feet either side of the joint, it seems pertinent to ask whether Westergaard's K is a significant index for the design for such pavements.

In a recent paper, Hveem (Figure 38 of reference 19) presents a view through a core hole in the pavement slab which shows approximately 1/4 inch clearance between the slab bottom and the subbase. The slab also shows a crack in this area. In reference to this illustration, Hveem states, "The existence of this space 'sets the stage' for pumping. There is reason to believe that the so-called pumping action could never start if the slab were firmly in contact with the subgrade at all times."

# Part II

## Theories of Stresses and Deflections in Concrete Roads Caused by Variations of Temperature

In the past, engineers have recognized the possibility of the loss of subgrade support at the corner of a slab resulting from moisture and temperature differentials. Older (29), in 1924, derived an equation for the required thickness of a concrete slab assuming that the corner was entirely unsupported. This "corner formula" was subsequently refined by Westergaard (49), Kelley (23), Spangler (36), Bradbury ( 5 ), and Pickett (31). However, as previously noted, there are few breaks of this type currently found in highway pavements. According to Sutherland (40), this is not only true of modern pavements but also of older pavements that are still in use.

In 1925, through the initiative of A. T. Goldbeck, then Chief of the Division of Tests in the Bureau of Public Roads, H. M. Westergaard was engaged to make theoretical studies of the structural action of pavements due to various types of loading (47). In 1927, Dr. Westergaard supplemented his earlier work by analyzing the stresses and deflections induced in slabs by temperature variations.

To obtain solutions, Westergaard made use of the following simplifying assumptions:

1) The slab is a homogeneous, isotropic, elastic solid of uniform thickness.

2) The slab is of infinite length and finite width.

3) The subgrade provides full and continuous support to the pavement at all points and all times.

4) The reaction of the subgrade is vertical and proportional to the deflections of the slab.

5) The temperature gradient increases linearly with the depth of the slab and remains constant on all planes parallel to the upper and lower slab surfaces.

In reference to Westergaard's analysis, Sutherland (40), in 1956, writes:

> At the time that this analysis was made it was not realized that the temperature differentials that develop in concrete pavements are as large as they are. After seeing some of the temperature differential data obtained in the Arlington investigation (23), Mr. Westergaard expressed the opinion that his analysis might not be applicable for temperature differentials of these magnitudes.

In 1940, J. Thomlinson (43), modified Westergaard's approach by assuming a simple harmonic temperature variation at the top surface of the slab, rather than a uniform temperature gradient in the slab. Applying the laws of heat flow, Thomlinson arrived at a curved temperature gradient through the depth of the slab which corresponds fairly closely with the cyclic daily observations of Teller and Sutherland (41), and Lang(24). However, as was previously noted, Teller and Sutherland concluded that although the curved gradient represents the more usual distribution of temperature, the straight line gradient defines the most critical stress condition caused by warping. Thus, it is not surprising that numerical values of the stresses computed by Thomlinson's analysis are less than those of Westergaard.

The analyses of Westergaard and Thomlinson represent the two major theories that have been developed for the calculation of warping stresses in concrete pavements due to temperature gradients. Both theories are predicated on full and intimate subgrade support. As

recent field studies have shown that this assumption may be seriously in error, the reliability of the stresses computed on this basis is open to question.

In spite of this fact, Westergaard's approach still remains an outstanding contribution to the problem of warping stresses in concrete pavements. Further analytical work need only be concerned with modifications of the simplifying assumptions to conform more closely to observed behavior. The fulfillment of this objective is the primary purpose of this thesis.

# THEORY

## Assumptions

1.) Slab is of circular shape, homogeneous and isotropic with a free edge boundary.

2.) Slab is supported on a homogeneous foundation.

3.) Reaction between slab and support at any point of contact is proportional to the deflection at that point.

4.) Slab obeys Hooke's law.

5.) Deflections of the slab are small in comparison with its thickness.

6.) Only external forces acting on the slab are those due to gravity.

7.) Slab is subject to ambient changes in temperature and/or moisture content which vary linearly with the depth of the slab but are constant on all planes parallel to the upper and lower slab surfaces.

## Formulation of Problem

The specific solution developed herein pertains to the case where the temperature and/or moisture content increases with the depth of the slab; consequently, the edges of the pavement will tend to warp up. The slab is divided into two zones (Figure 2 ) with the inner portion (zone 1) having a uniformly loaded slab on an elastic foundation while the outer region (zone 2) is unsupported by the foundation. Conditions of continuity require that along the circle of radius b, the deflection, slope, bending moment, and shear of both inner and outer portions be equal.

SIMPLIFIED DIAMETRAL SECTION OF WARPED SLAB

FIGURE 2

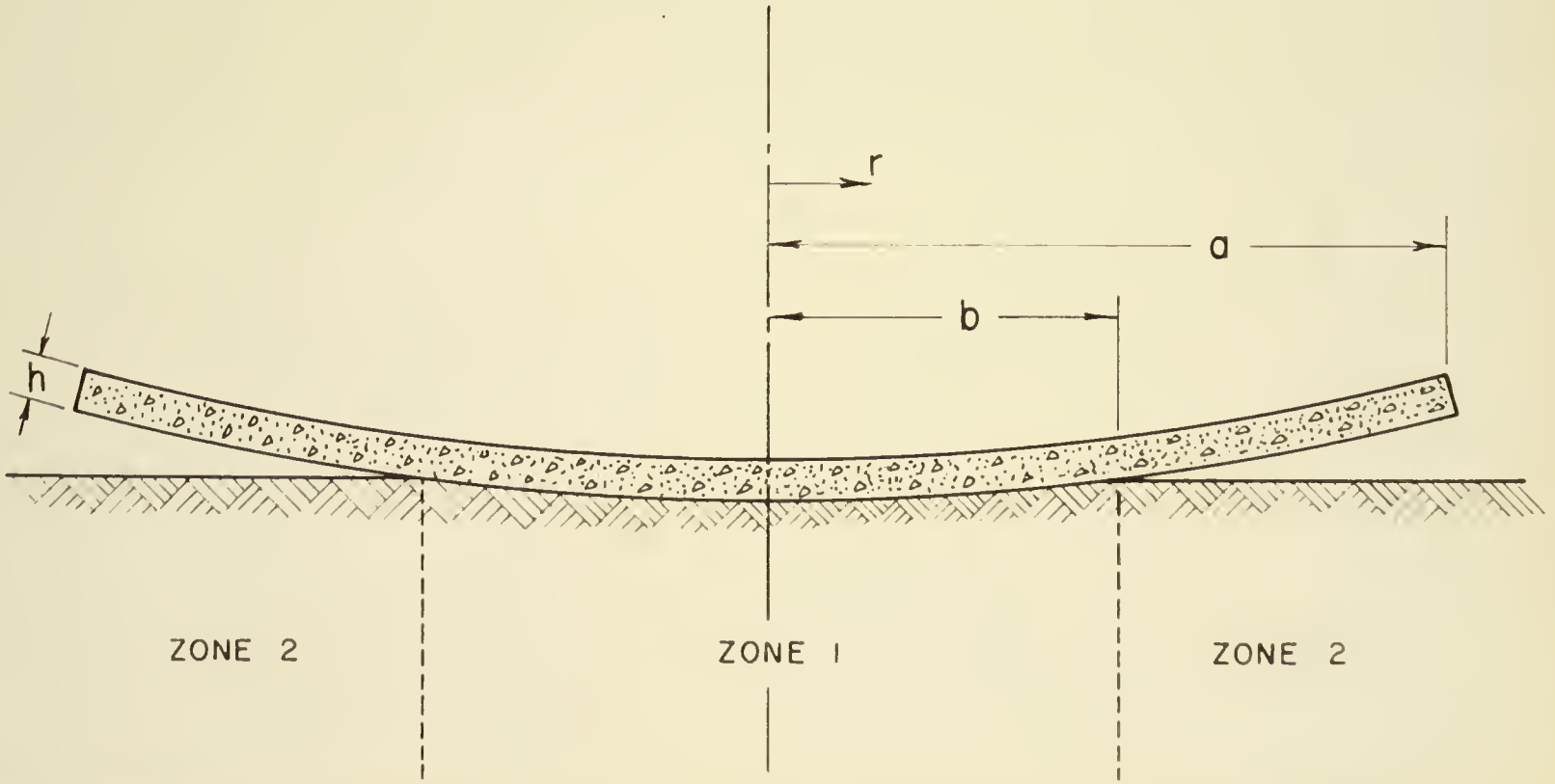

As the loading and reactive forces are symmetrically distributed about an axis perpendicular to the slab through its center, both the slope and the shear at the center of the slab must be zero.

The assumptions, boundary conditions, and symmetry may be summarized as follows (see nomenclature in Appendix I):

a) $w_1'(0) = 0$

b) $V_1(0) = 0$

c) $w_1(b) = 0$

d) $V_2(a) = 0$

e) $M_2(a) = 0$

f) $w_2(b) = 0$

g) $w_1'(b) = w_2'(b)$

h) $M_1(b) = M_2(b)$

i) $V_1(b) = V_2(b)$

## Solution of Problem

Applying the conditions listed above to the governing differential equations, the following equations for stresses and deflections in the slab are obtained (see Appendix II for derivation):

For $0 < r \leq b$ or $0 < \rho \leq \beta$,

$$\sigma_\rho = \frac{Eh}{2(1-\mu^2)} \left[ \frac{q}{K\ell^2} \left( C_1 \left[ Z_2(\rho) - \frac{(1-\mu)Z_1'(\rho)}{\rho} \right] - C_2 \left[ Z_1(\rho) + \frac{(1-\mu)Z_2'(\rho)}{\rho} \right] \right) + \alpha ( 1 + \mu ) \frac{T}{h} \right] \tag{19}$$

$$w_1(\rho) = \frac{q}{K} \left( 1 + C_1 Z_1(\rho) + C_2 Z_2(\rho) \right). \tag{9}$$

For $b \leq r \leq a$,

$$\sigma_r = \frac{Eh}{2(1-\mu)^2}\left[C_6(\mu-1)\left(\frac{1}{r^2} - \frac{1}{a^2}\right) + \frac{qa^2}{4D}(1+\mu)\ln\frac{a}{r} - \frac{q(3+\mu)}{16D}(a^2-r^2)\right) \quad (18)$$

$$w_2(r) = C_5 + C_6 \ln r + C_7 r^2 + C_8 r^2 \ln r + \frac{qr^4}{64D} \quad (5)$$

where

$$C_1 = -\frac{1 + C_2 Z_2(\beta)}{Z_1(\beta)} \quad (10)$$

$$\frac{C_6(\mu-1)}{a^2} + 2C_7(1+\mu) - \frac{qa^2}{16D}[4(\mu+1)\ln a + (3+\mu)] + \alpha(1+\mu)\frac{T}{h} = 0 \quad (13)$$

$$C_5 + C_6 \ln b + C_7 b^2 - \frac{qa^2b^2\ln b}{8D} + \frac{qb^4}{64D} = 0 \quad (14)$$

$$\frac{C_6}{b} + 2C_7 b - \frac{qa^2 b}{8D}(2\ln b + 1) + \frac{qb^3}{16D} - \frac{q}{K\ell}[C_1 Z_1'(\beta) + C_2 Z_2'(\beta)] = 0 \quad (15)$$

$$\frac{C_6}{b^2}(\mu-1) + 2C_7(1+\mu) - \frac{qa^2}{8D}[2(1+\mu)\ln b + (3+\mu)] + \frac{qb^2}{16D}(3+\mu)$$

$$- \frac{q}{K\ell^2}\left\{C_1\left[Z_2(\beta) - \frac{(1-\mu)Z_1'(\beta)}{\beta}\right] - C_2\left[Z_1(\beta) + \frac{(1-\mu)Z_2'(\beta)}{\beta}\right]\right\} = 0 \quad (16)$$

$$C_2 = -\left\{\frac{Z_2'(\beta) - Z_1(\beta)[a^2-b^2]\frac{1}{2b\ell}}{Z_2(\beta)Z_2'(\beta) + Z_1'(\beta)Z_1(\beta)}\right\}. \quad (17)$$

An examination of these equations shows that a prohibitive amount of work would be required to eliminate the constants and then obtain an

explicit expression for either the stresses or deflections in terms of the slab parameters. In the early stages of this study, form sheets were prepared and used to simplify the computations. Appendix III contains a typical set of calculations as computed by hand calculator. To evaluate the effects of various combinations of factors that are of interest, it was estimated that these calculations would have to be repeated several hundred times. Thus, it was decided that a high-speed calculator was essential to obtain the desired information within a reasonable period of time.

## Digital Computer

The problem was programmed for the Datatron 204 digital computer at Purdue University. As a part of the solution, subroutines were developed for the Ber ($\rho$) and Bei ($\rho$) functions and their first derivatives (see Appendix V).

The main program (see Appendix IV) was written with b, the radial distance to the point of zero deflection, as the independent variable; and T, the effective temperature difference between the slab surfaces, as the dependent variable.

Initially, the program was set up such that by introducing a set of parameters (a, K, E, h, etc.), the computer would solve for T corresponding to the condition b = a, and then, print out the stresses and deflections at equal radial increments across the slab. Repeating the cycle with decrements in b, the stresses and deflections were computed for a range of temperature differentials.

It soon became apparent that it would be more advantageous if T was the independent variable. An examination of the equations showed

that it would be impractical to solve for b as a function of T. However, by virtue of the speed of the computer, a modification was written which effectively transformed the initial program to one with T as the independent variable. If the stresses and deflections were desired for a temperature differential of $30^{\circ}$, the computer would choose b = a and solve for T as before. The resulting T would then be compared with $30^{\circ}$. If the T value was less than $30^{\circ}$, the computer would select a lower value of b and solve for the corresponding T. The cycle would repeat until a T greater than $30^{\circ}$ resulted. The computer would then back-step a fraction of the decrement and recycle. By repeating the procedure, T could be obtained to any degree of precision. Having the corresponding b value, the stresses and deflections were readily computed. On the average, 45 seconds were required to obtain b for any T; during this time, the computer recycled approximately 15 times.

## RESULTS

The derived equations were solved for deflections and (normal) radial stresses for combinations of the following:*

$E = 3 \times 10^6$, $4 \times 10^6$, $5 \times 10^6$ psi

a = 80", 120", 160", 200", 220", 240"

h = 4", 6", 8", 10", 12", 14", 16", 18", 20", 24"

K = 100, 200, 400, 700 pci

$T = 20^\circ$, $30^\circ$, $40^\circ$ F

$\alpha = 6 \times 10^{-6}$ inches per inch per $^\circ$F

$\mu = 0.15$

Typical deflection curves for an effective temperature difference between slab surfaces of $30^\circ$F are shown in Figure 3. Corresponding radial stresses as a function of the radial distance from the center of the slab are shown in Figure 4.

Ratios of the maximum radial stress ($\sigma$ max.) to the stress at the center of the slab ($\sigma_o$) were computed for combinations of the following parameters:

$E = 3 \times 10^6$, $5 \times 10^6$ psi

a = 120", 240"

K = 100, 200, 400, 700 pci

h = 4", 8", 12", 16", 24"

The results are presented in Table 1, which shows that for a = 240" there is little loss in precision by assuming the central stress equivalent to the maximum stress; for a = 120", the central stress is the maximum. As

---

*See page 59 for list of symbols.

REPRESENTATIVE DEFLECTION CURVES FOR AN EFFECTIVE TEMPERATURE DIFFERENCE OF 30° F. BETWEEN SLAB SURFACES

FIGURE 3

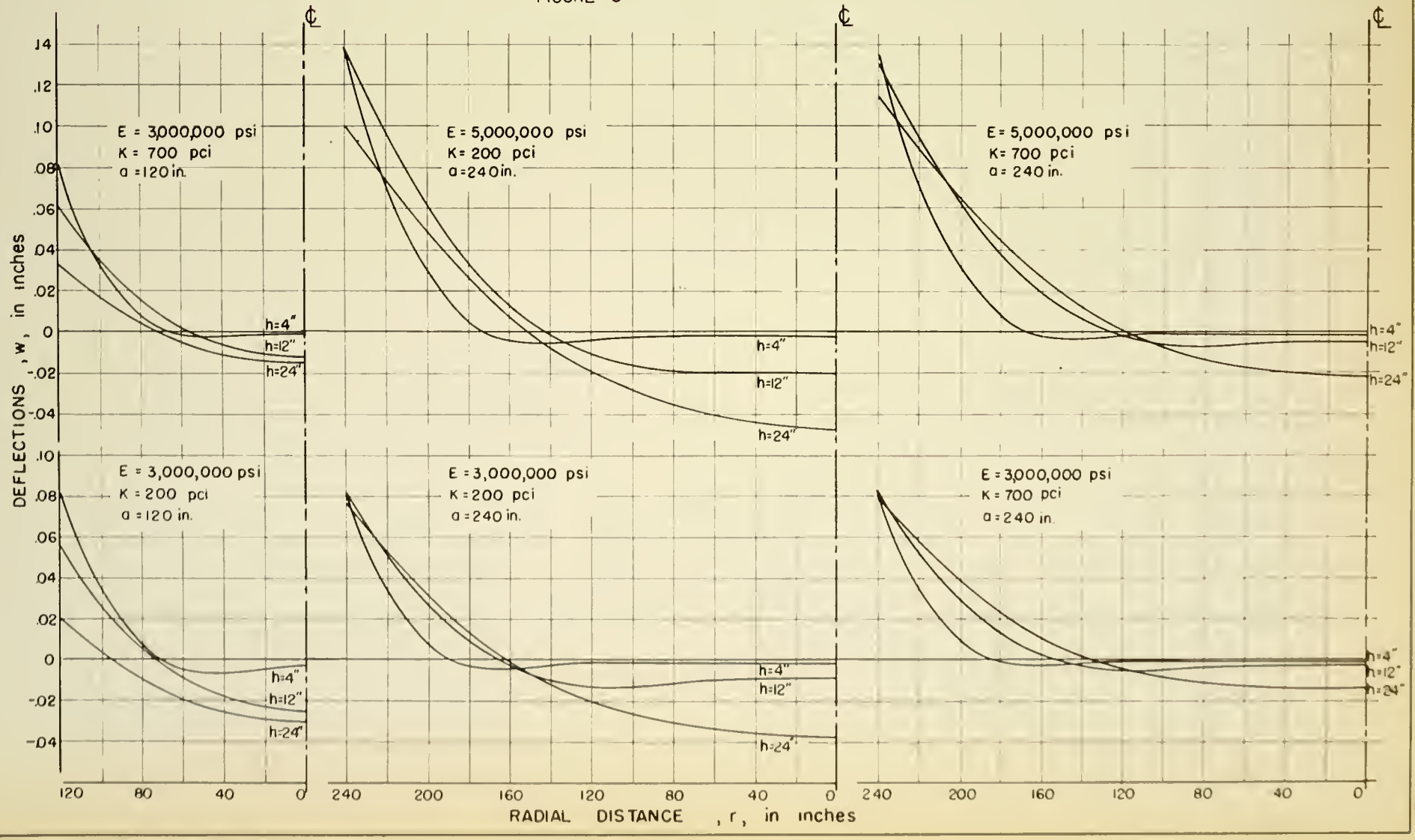

REPRESENTATIVE RADIAL STRESSES FOR AN EFFECTIVE TEMPERATURE DIFFERENCE OF 30° F. BETWEEN SLAB SURFACES

FIGURE 4

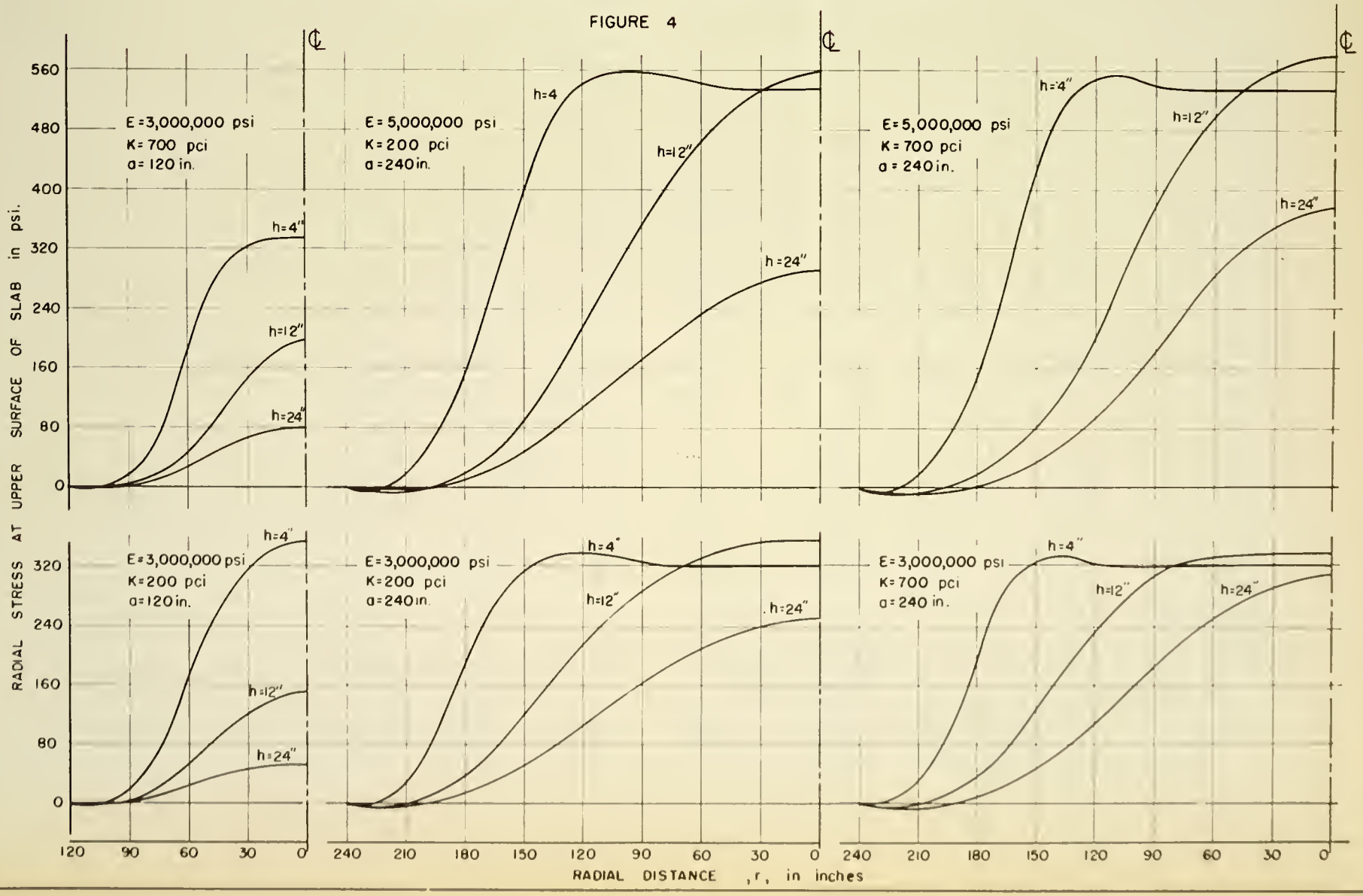

REPRESENTATIVE RATIOS OF THE MAXIMUM RADIAL STRESS ( $\sigma_r$ max.) TO THE NORMAL STRESS AT THE CENTER OF THE SLAB ($\sigma_o$)

TABLE I

E = 3,000,000 psi , a = 240 in. , T = 30° F.

| h (in.) \ K (pci) | 100 | 200 | 400 | 700 |
|---|---|---|---|---|
| 4 | 1.049 | 1.041 | 1.035 | 1.031 |
| 8 | 1.000 | 1.020 | 1.040 | 1.044 |
| 12 | 1.000 | 1.000 | 1.000 | 1.001 |
| 16 | 1.000 | 1.000 | 1.000 | 1.000 |

E = 5,000,000 psi , a = 240 in. , T = 30° F

| h (in.) \ K (pci) | 100 | 200 | 400 | 700 |
|---|---|---|---|---|
| 4 | 1.048 | 1.045 | 1.037 | 1.032 |
| 8 | 1.000 | 1.000 | 1.001 | 1.013 |
| 12 | 1.000 | 1.000 | 1.000 | 1.000 |

For a = 120 inches $\sigma_r$ max. = $\sigma_o$ for all computed conditions.

several minutes of computer time were required to calculate the maximum stress, whereas the time required to obtain the stress at the center could be measured in milliseconds, this latter stress was used in lieu of the maximum stress in the analyses to follow. In no case is the error greater than 5%.

Tables 2 and 3 contain typical upward edge deflections and radial distances (b) to points of unsupport.

The calculated stress relationships are shown in the form of charts in Figures 5A to 5L. These relationships are plots of the ratios of the central stress ($\sigma_o$) to the modulus of rupture ($M_r$) for effective temperature differences of 20°F, 30°F, 40°F, and for various combinations of slab radii (a) and thicknesses (h). The use of these curves can best be illustrated by an example. For a stress ratio ($\sigma_o/M_r$) of 0.5, E = $3 \times 10^6$ psi, K = 100 pci, and with an anticipated effective temperature gradient of 30°F, (following the arrows in Figure 5A) the curves show that among the various possible solutions are a 134" radius slab, 8" thick and a 211" radius slab, 16" thick. The relationship between the moduli of rupture and elasticity were obtained from references (21 and 27) and are plotted in Figure 6.

The data for a = 240", T = 30°F are cross-plotted on Figure 7 to illustrate the effects of the quality of the concrete in the slab as characterized by the modulus of elasticity, E. Figure 8 shows the effects of increasing effective temperature differences.

## REPRESENTATIVE UPWARD EDGE DEFLECTIONS (T = 30°F.)

TABLE 2

E = 3,000,000 psi — a = 240 in. — E = 5,000,000 psi

| h(in) \ K(pci) | 100 | 200 | 400 | 700 | 100 | 200 | 300 | 700 |
|---|---|---|---|---|---|---|---|---|
| 4 | 0.079 | 0.080 | 0.080 | 0.080 | 0.130 | 0.133 | 0.137 | 0.134 |
| 8 | 0.079 | 0.077 | 0.082 | 0.078 | 0.132 | 0.131 | 0.138 | 0.137 |
| 12 | 0.078 | 0.081 | 0.081 | 0.082 | 0.137 | 0.135 | 0.133 | 0.130 |
| 16 | 0.075 | 0.080 | 0.082 | 0.079 | 0.117 | 0.125 | 0.128 | 0.127 |
| 24 | 0.061 | 0.075 | 0.078 | 0.079 | 0.083 | 0.097 | 0.111 | 0.115 |

E = 3,000,000 psi — a = 120 in. — E = 5,000,000 psi

| h(in) \ K(pci) | 100 | 200 | 400 | 700 | 100 | 200 | 300 | 700 |
|---|---|---|---|---|---|---|---|---|
| 4 | 0.080 | 0.081 | 0.079 | 0.080 | 0.127 | 0.127 | 0.128 | 0.126 |
| 8 | 0.069 | 0.075 | 0.076 | 0.074 | 0.083 | 0.091 | 0.096 | 0.099 |
| 12 | 0.045 | 0.053 | 0.059 | 0.062 | 0.050 | 0.061 | 0.068 | 0.070 |
| 16 | 0.028 | 0.039 | 0.046 | 0.049 | 0.030 | 0.041 | 0.049 | 0.054 |
| 24 | 0.006 | 0.019 | 0.030 | 0.032 | 0.007 | 0.019 | 0.028 | 0.033 |

REPRESENTATIVE RADIAL DISTANCES (b) TO POINTS OF UNSUPPORT

TABLE 3

E = 3,000,000 psi  a = 240 in.  E = 5,000,000 psi

| h (in.) \ K (pci) | 100 | 200 | 400 | 700 | 100 | 200 | 400 | 700 |
|---|---|---|---|---|---|---|---|---|
| 4 | 194.89 | 190.45 | 186.67 | 184.00 | 178.00 | 172.67 | 168.00 | 165.33 |
| 8 | 184.00 | 177.11 | 170.00 | 166.44 | 162.00 | 154.00 | 146.00 | 141.33 |
| 12 | 178.00 | 168.00 | 160.00 | 154.00 | 154.00 | 142.44 | 133.33 | 127.33 |
| 16 | 176.00 | 162.67 | 152.00 | 146.00 | 157.33 | 140.67 | 127.33 | 118.59 |
| 24 | 183.33 | 162.67 | 146.67 | 136.00 | 172.67 | 150.44 | 130.67 | 117.56 |

E = 3,000,000 psi  a = 120 in.  E = 5,000,000 psi

| h(in.) \ K (pci) | 100 | 200 | 400 | 700 | 100 | 200 | 400 | 700 |
|---|---|---|---|---|---|---|---|---|
| 4 | 76.44 | 72.00 | 68.67 | 66.00 | 63.70 | 58.37 | 53.93 | 51.19 |
| 8 | 75.78 | 66.89 | 59.78 | 55.11 | 71.04 | 61.33 | 53.16 | 47.41 |
| 12 | 85.04 | 73.48 | 63.70 | 56.89 | 82.49 | 70.44 | 60.27 | 53.16 |
| 16 | 94.82 | 81.11 | 69.56 | 61.56 | 93.33 | 79.33 | 67.48 | 59.26 |
| 24 | 113.11 | 96.00 | 81.78 | 71.70 | 112.30 | 95.11 | 80.59 | 70.44 |

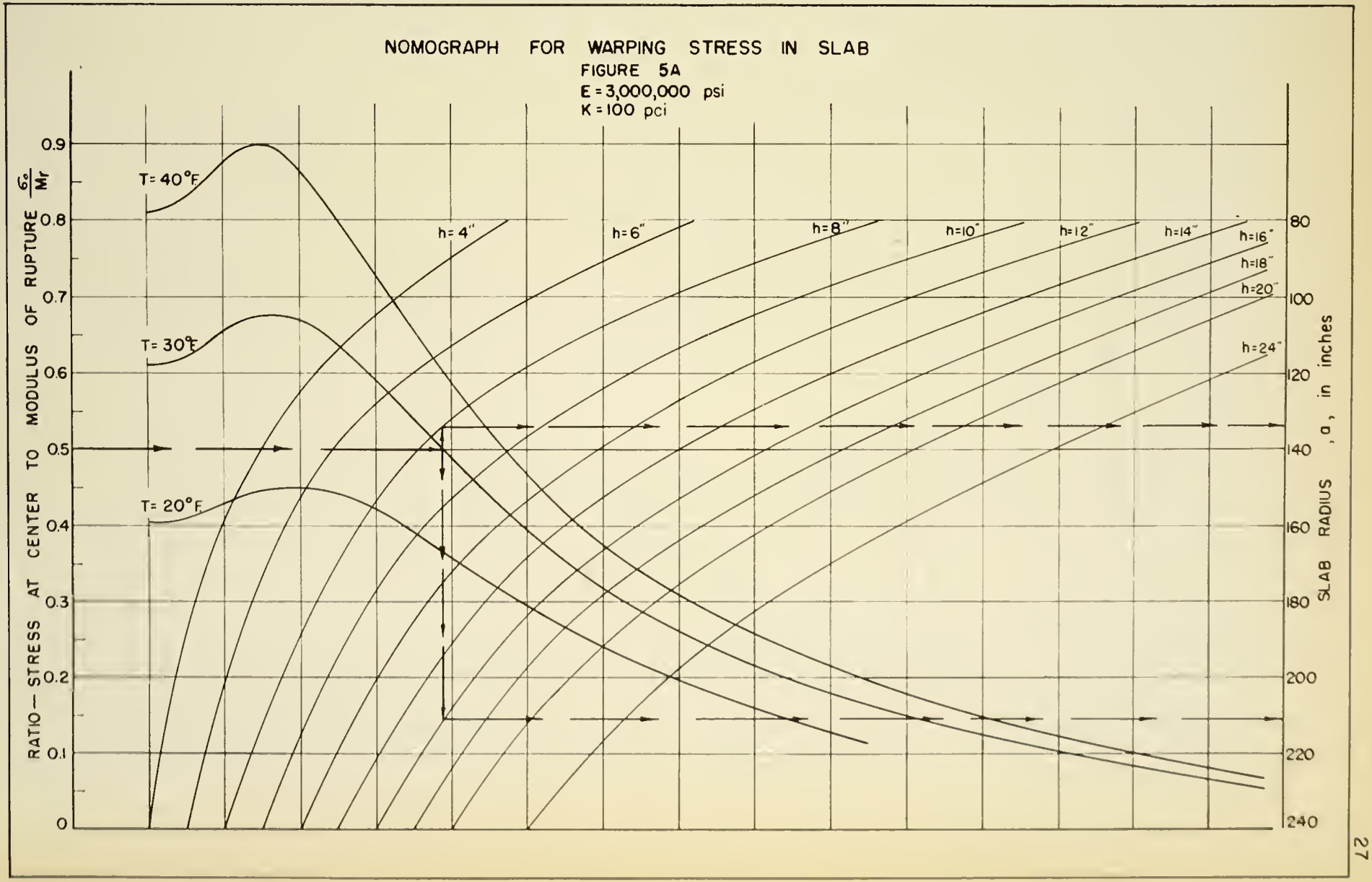
NOMOGRAPH FOR WARPING STRESS IN SLAB
FIGURE 5A
E = 3,000,000 psi
K = 100 pci
RATIO — STRESS AT CENTER TO MODULUS OF RUPTURE σc/Mr
SLAB RADIUS, a, in inches
0
0.1
0.2
0.3
0.4
0.5
0.6
0.7
0.8
0.9
80
100
120
140
160
180
200
220
240
T= 40°F
T= 30°F
T= 20°F
h= 4"
h= 6"
h= 8"
h=10"
h=12"
h=14"
h=16"
h=18"
h=20"
h=24"

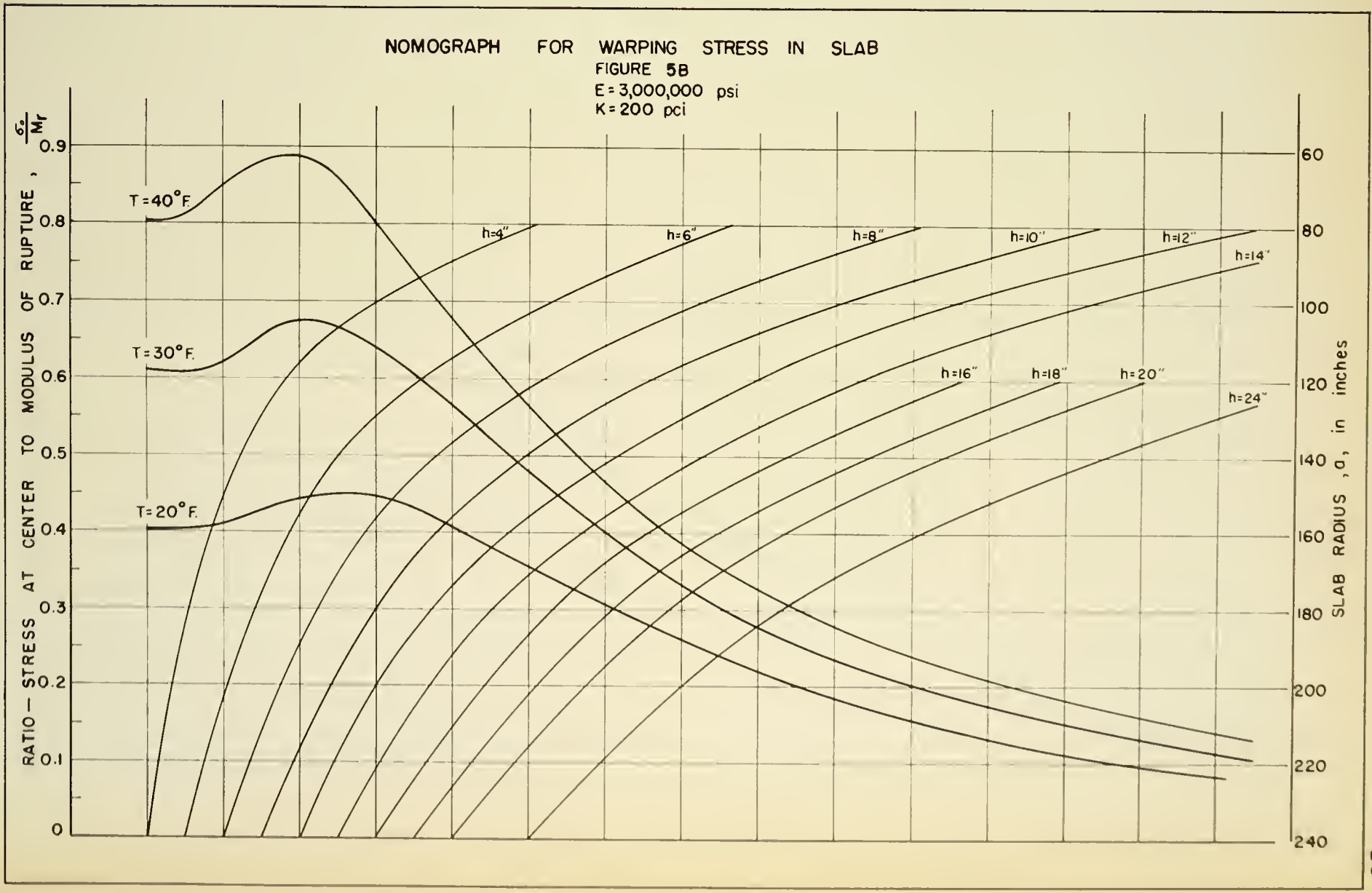
NOMOGRAPH FOR WARPING STRESS IN SLAB
FIGURE 5B
E = 3,000,000 psi
K = 200 pci
RATIO — STRESS AT CENTER TO MODULUS OF RUPTURE, σc/Mr
SLAB RADIUS, a, in inches
0
0.1
0.2
0.3
0.4
0.5
0.6
0.7
0.8
0.9
60
80
100
120
140
160
180
200
220
240
T = 40° F.
T = 30° F.
T = 20° F.
h=4"
h=6"
h=8"
h=10"
h=12"
h=14"
h=16"
h=18"
h=20"
h=24"

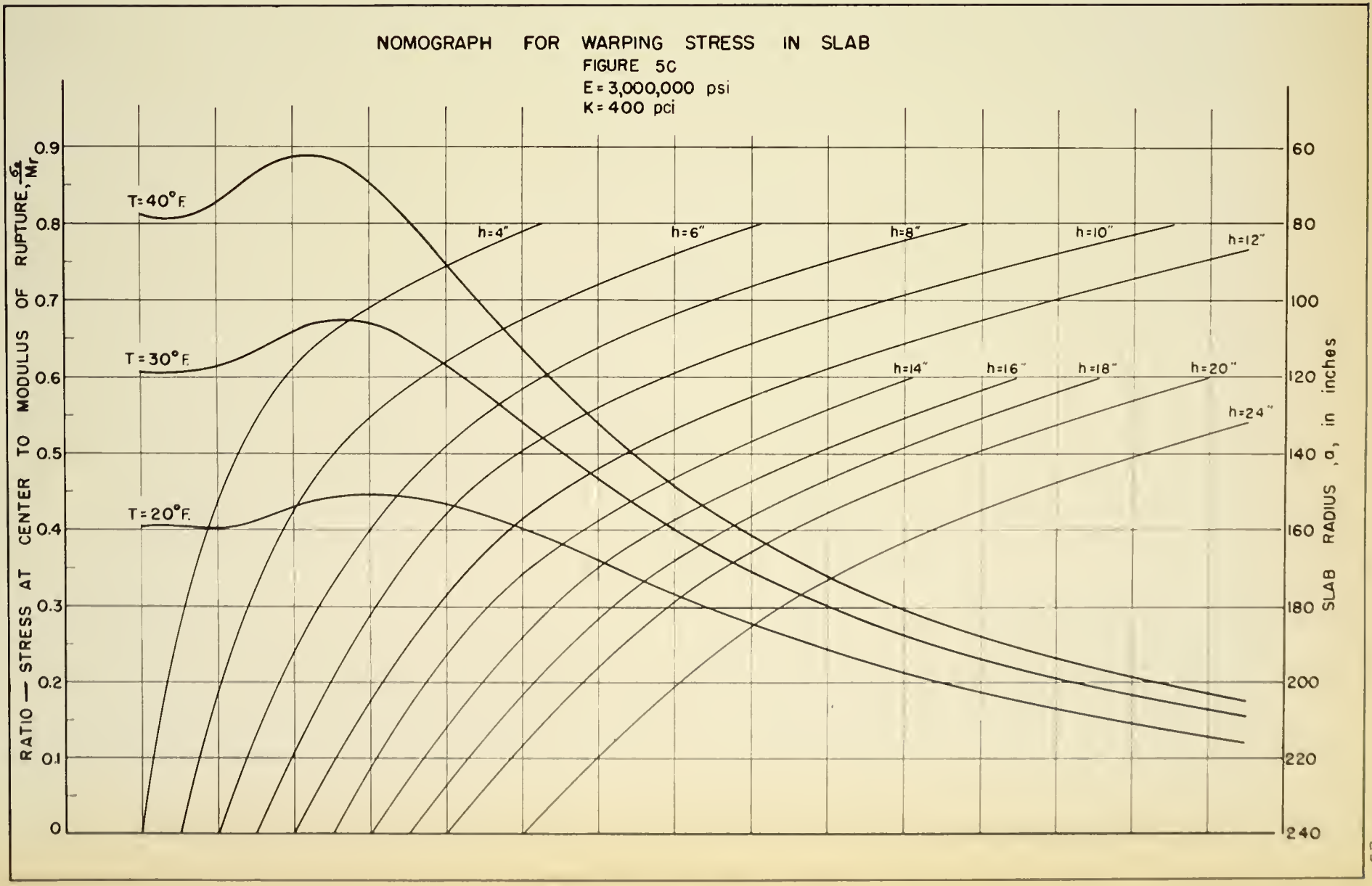
NOMOGRAPH FOR WARPING STRESS IN SLAB
FIGURE 5C
E = 3,000,000 psi
K = 400 pci
RATIO — STRESS AT CENTER TO MODULUS OF RUPTURE, σa/Mr
SLAB RADIUS, a, in inches
T=40°F.
T=30°F.
T=20°F.
h=4"
h=6"
h=8"
h=10"
h=12"
h=14"
h=16"
h=18"
h=20"
h=24"
0
0.1
0.2
0.3
0.4
0.5
0.6
0.7
0.8
0.9
60
80
100
120
140
160
180
200
220
240

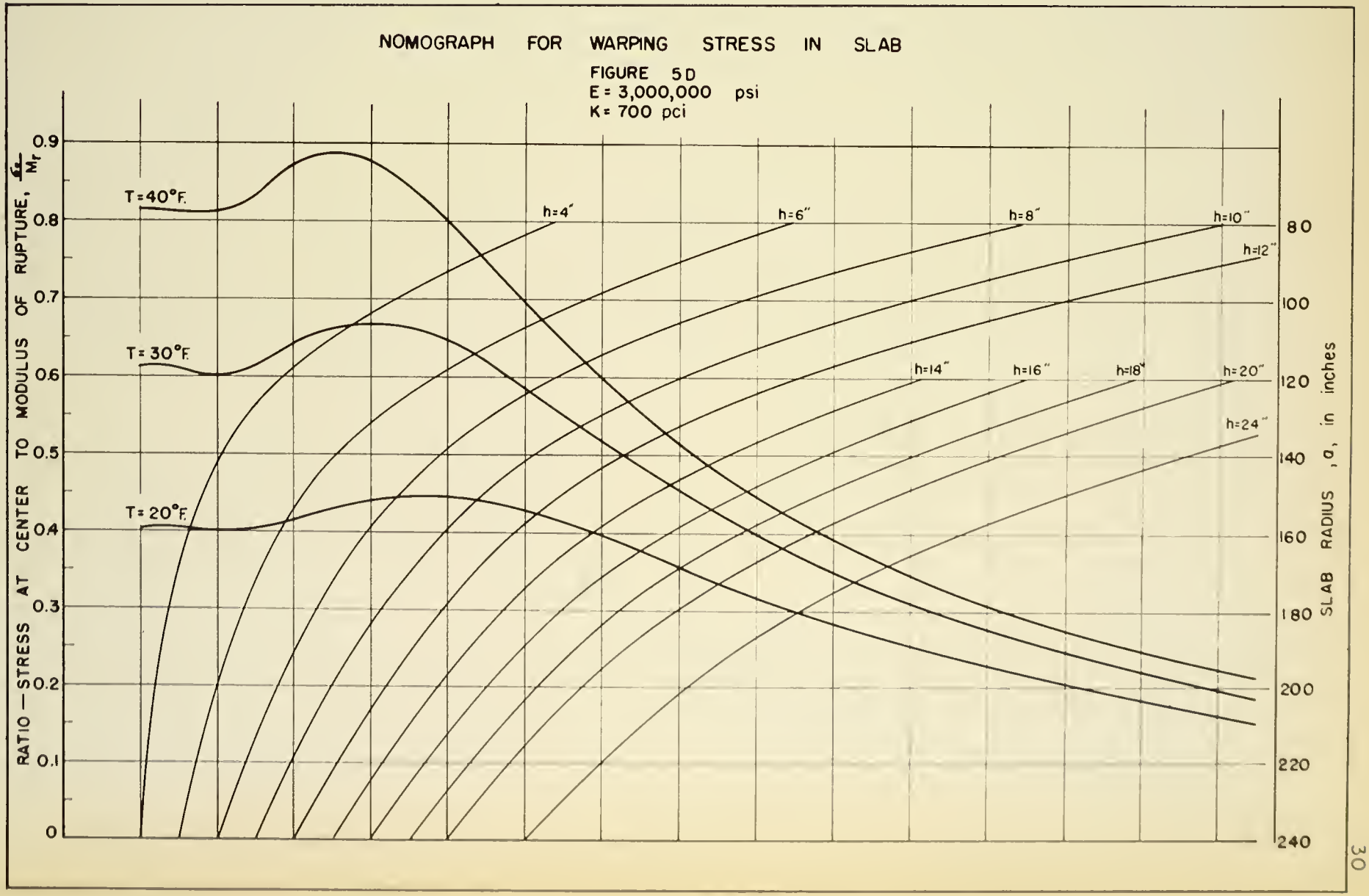
NOMOGRAPH FOR WARPING STRESS IN SLAB
FIGURE 5D
E = 3,000,000 psi
K = 700 pci
RATIO — STRESS AT CENTER TO MODULUS OF RUPTURE, $\frac{\sigma_c}{M_r}$
SLAB RADIUS, a, in inches
T=40°F.
T=30°F.
T=20°F.
h=4"
h=6"
h=8"
h=10"
h=12"
h=14"
h=16"
h=18"
h=20"
h=24"
0
0.1
0.2
0.3
0.4
0.5
0.6
0.7
0.8
0.9
80
100
120
140
160
180
200
220
240

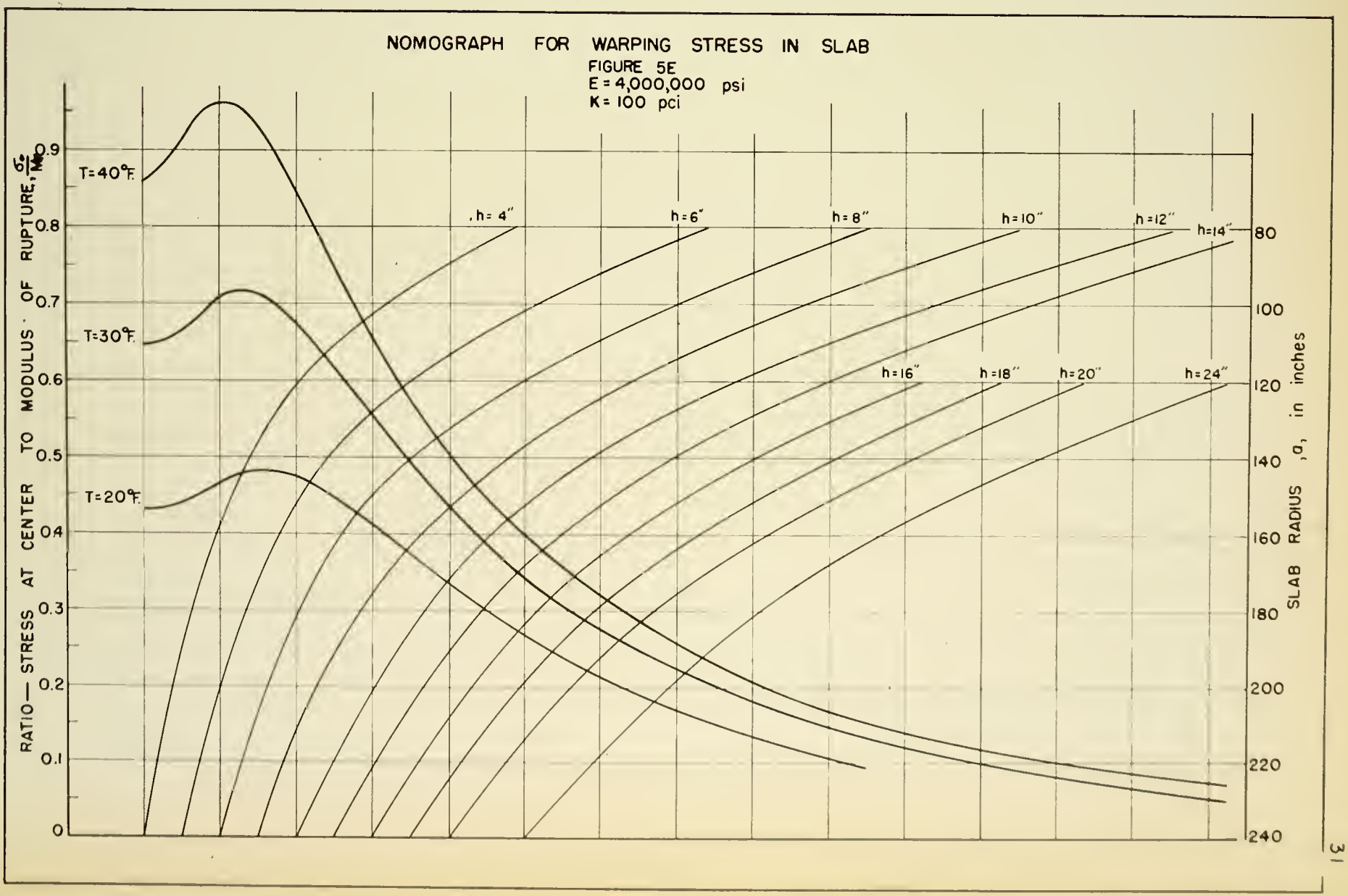
NOMOGRAPH FOR WARPING STRESS IN SLAB
FIGURE 5E
E = 4,000,000 psi
K = 100 pci
RATIO — STRESS AT CENTER TO MODULUS OF RUPTURE, σc/MR
SLAB RADIUS, a, in inches
T=40°F.
T=30°F.
T=20°F.
h = 4"
h = 6"
h = 8"
h = 10"
h = 12"
h = 14"
h = 16"
h = 18"
h = 20"
h = 24"
0
0.1
0.2
0.3
0.4
0.5
0.6
0.7
0.8
0.9
80
100
120
140
160
180
200
220
240

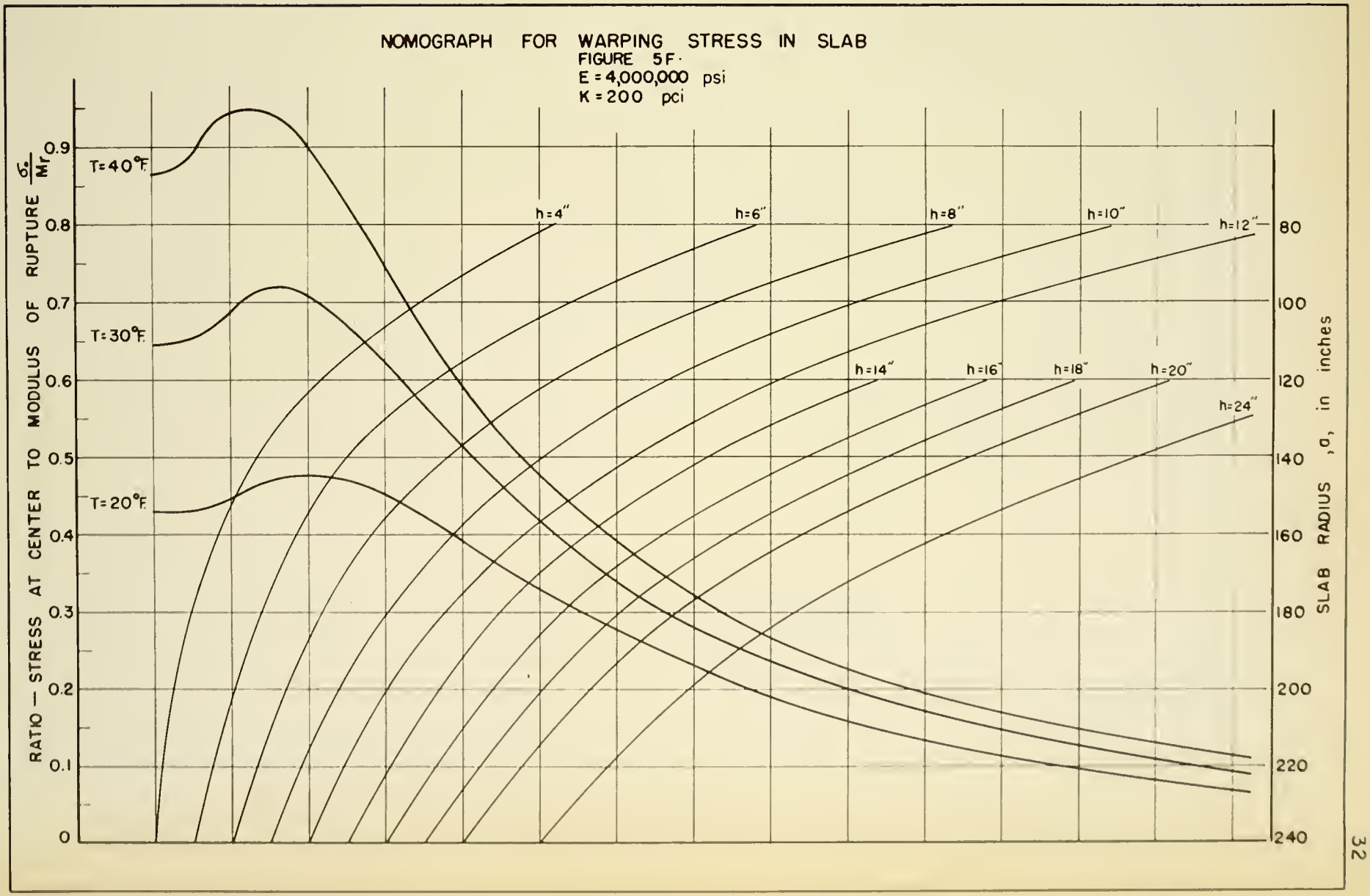
NOMOGRAPH FOR WARPING STRESS IN SLAB
FIGURE 5F.
E = 4,000,000 psi
K = 200 pci
RATIO — STRESS AT CENTER TO MODULUS OF RUPTURE σc/Mr
SLAB RADIUS, a, in inches
T=40°F.
T=30°F.
T=20°F.
h=4"
h=6"
h=8"
h=10"
h=12"
h=14"
h=16"
h=18"
h=20"
h=24"
0
0.1
0.2
0.3
0.4
0.5
0.6
0.7
0.8
0.9
80
100
120
140
160
180
200
220
240

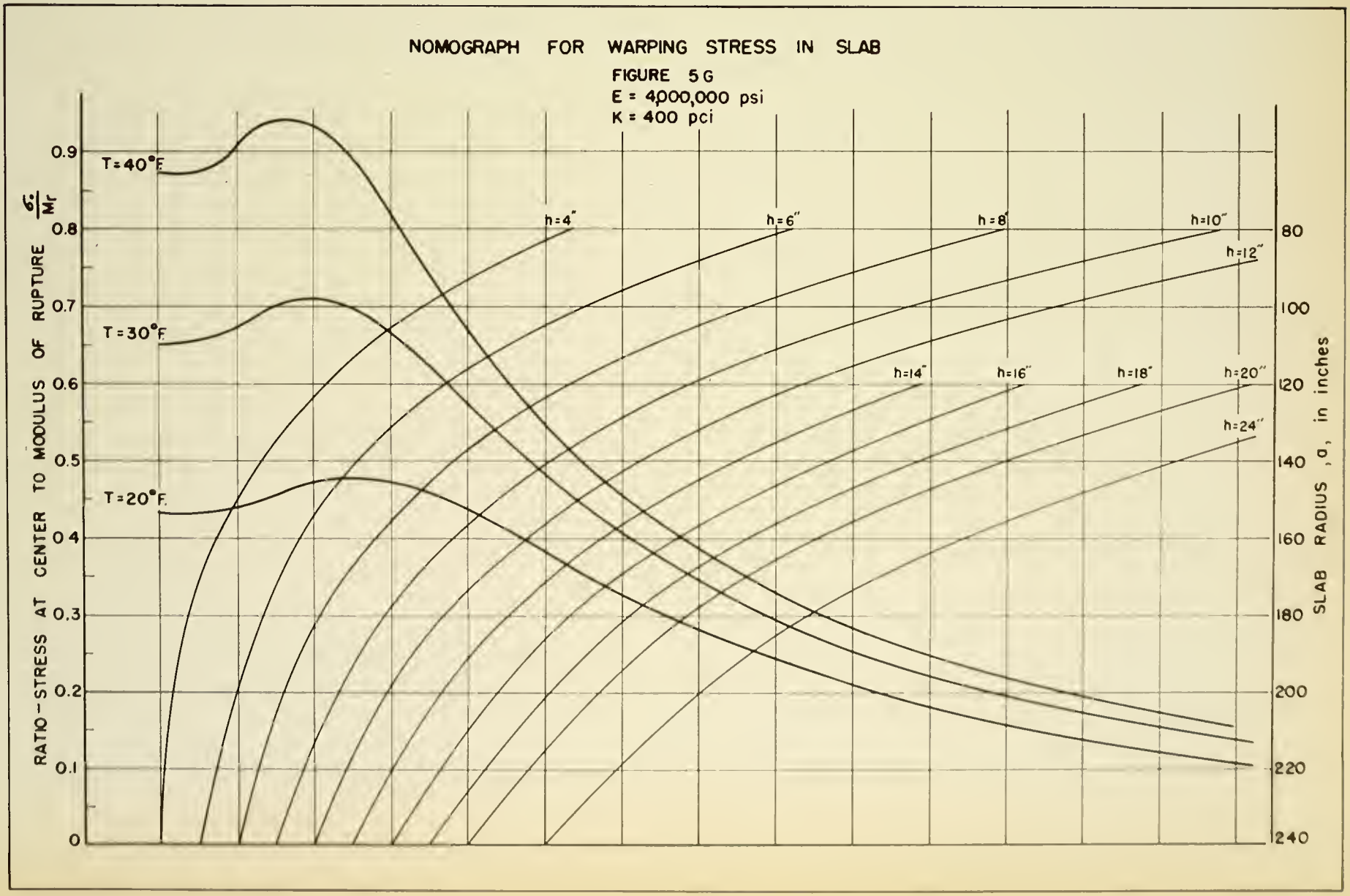
NOMOGRAPH FOR WARPING STRESS IN SLAB
FIGURE 5G
E = 4,000,000 psi
K = 400 pci
RATIO - STRESS AT CENTER TO MODULUS OF RUPTURE σc/Mr
SLAB RADIUS, a, in inches
T=40°F
T=30°F
T=20°F
h=4"
h=6"
h=8"
h=10"
h=12"
h=14"
h=16"
h=18"
h=20"
h=24"
0
0.1
0.2
0.3
0.4
0.5
0.6
0.7
0.8
0.9
80
100
120
140
160
180
200
220
240

## NOMOGRAPH FOR WARPING STRESS IN SLAB

FIGURE 5H
E=4,000,000 psi
K=700 pci

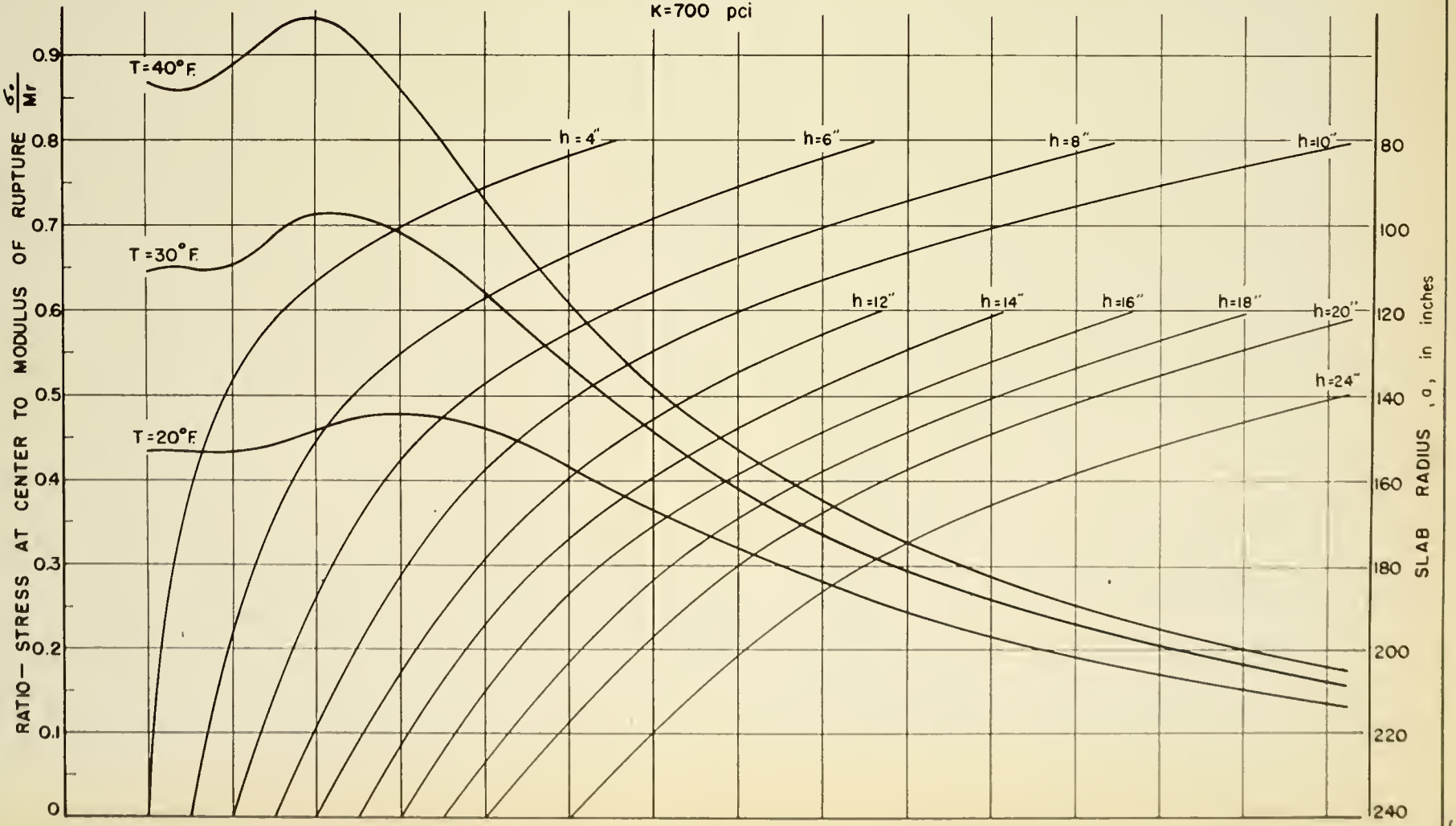

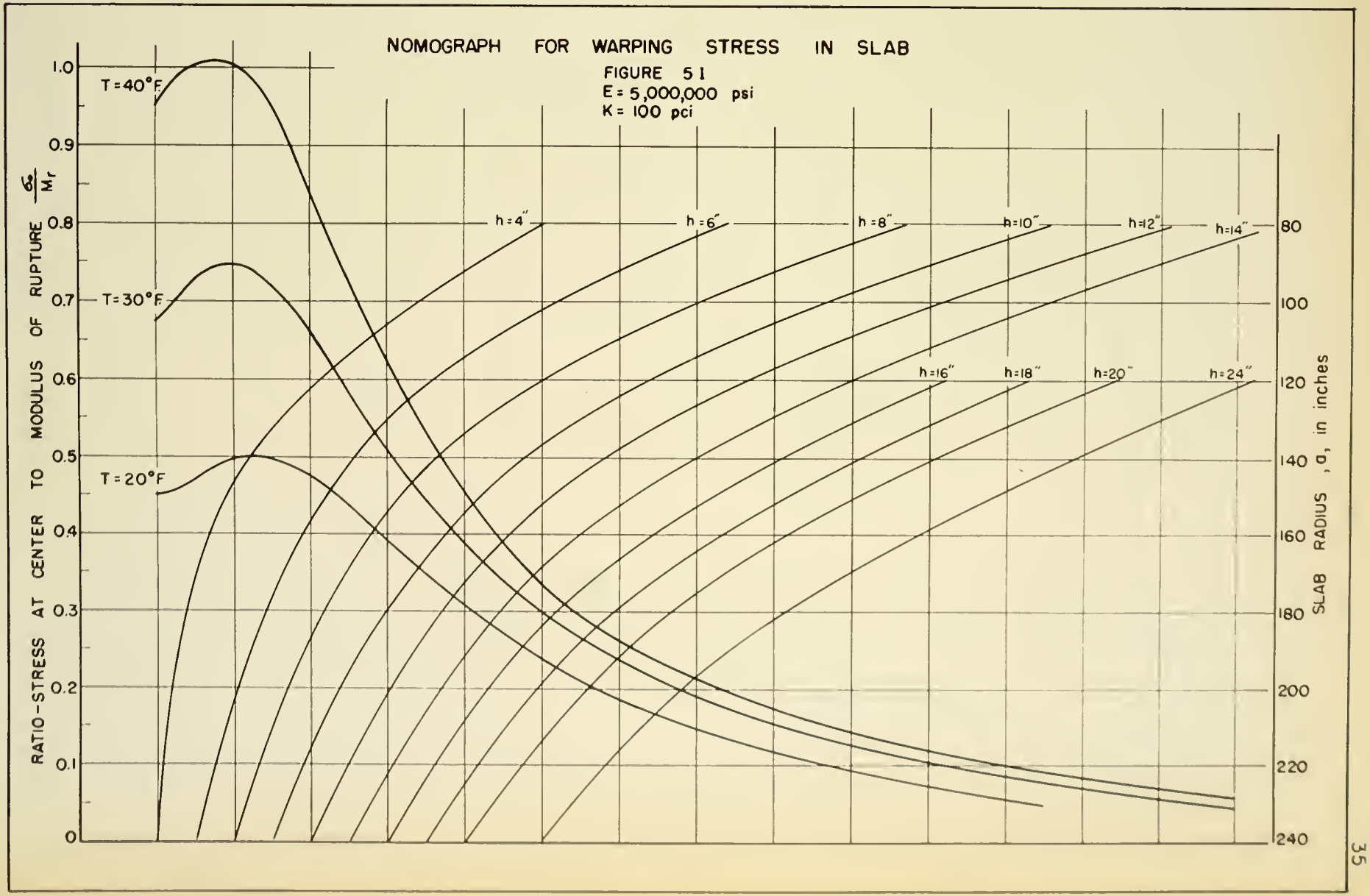
NOMOGRAPH FOR WARPING STRESS IN SLAB
FIGURE 51
E = 5,000,000 psi
K = 100 pci
RATIO-STRESS AT CENTER TO MODULUS OF RUPTURE σ/Mr
SLAB RADIUS, a, in inches
T=40°F
T=30°F
T=20°F
h=4"
h=6"
h=8"
h=10"
h=12"
h=14"
h=16"
h=18"
h=20"
h=24"
1.0
0.9
0.8
0.7
0.6
0.5
0.4
0.3
0.2
0.1
0
80
100
120
140
160
180
200
220
240

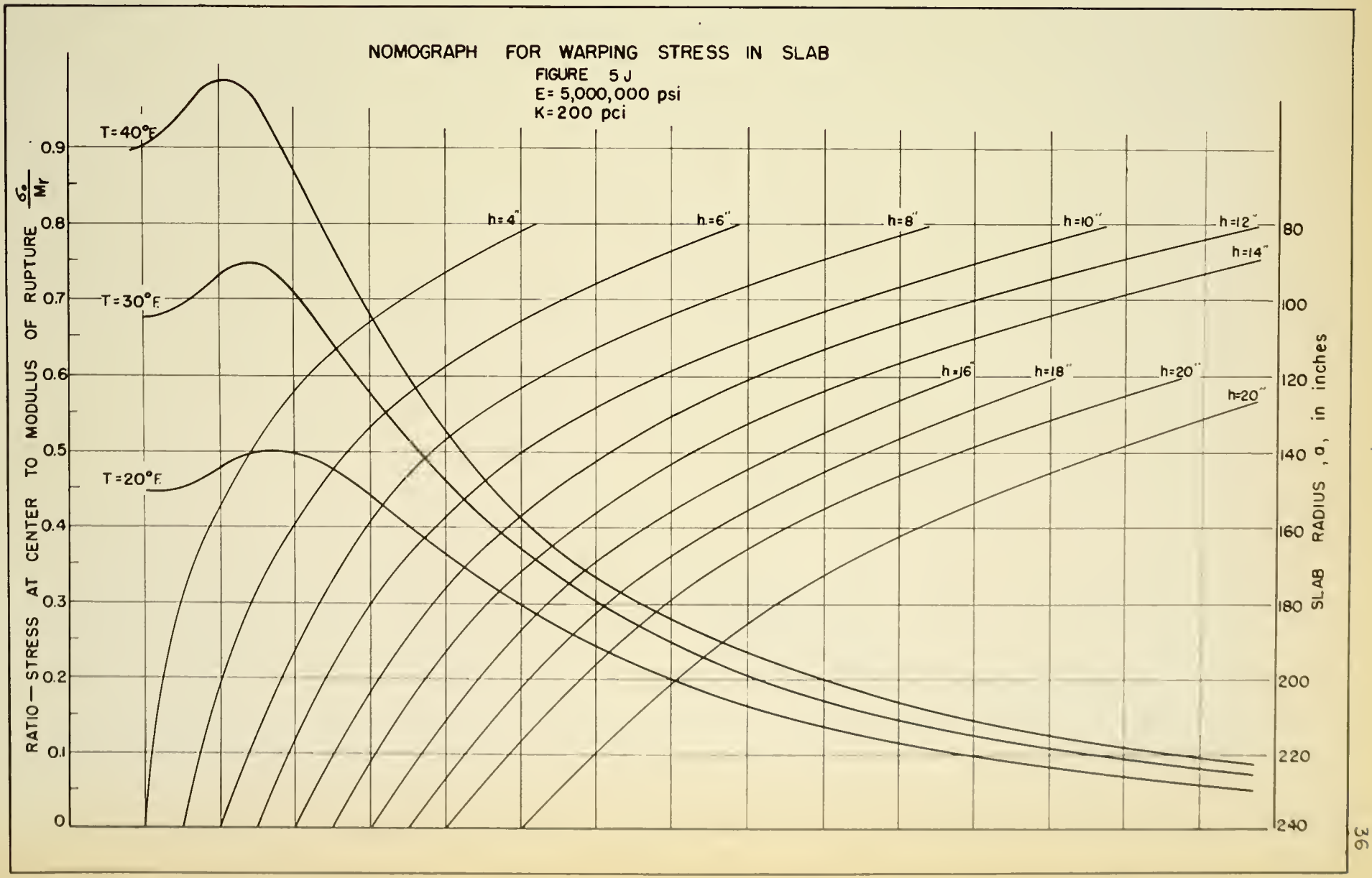
NOMOGRAPH FOR WARPING STRESS IN SLAB
FIGURE 5 J
E = 5,000,000 psi
K = 200 pci
RATIO — STRESS AT CENTER TO MODULUS OF RUPTURE σc/Mr
SLAB RADIUS, a, in inches
T = 40°F
T = 30°F
T = 20°F
h = 4"
h = 6"
h = 8"
h = 10"
h = 12"
h = 14"
h = 16"
h = 18"
h = 20"
h = 20"
0
0.1
0.2
0.3
0.4
0.5
0.6
0.7
0.8
0.9
80
100
120
140
160
180
200
220
240

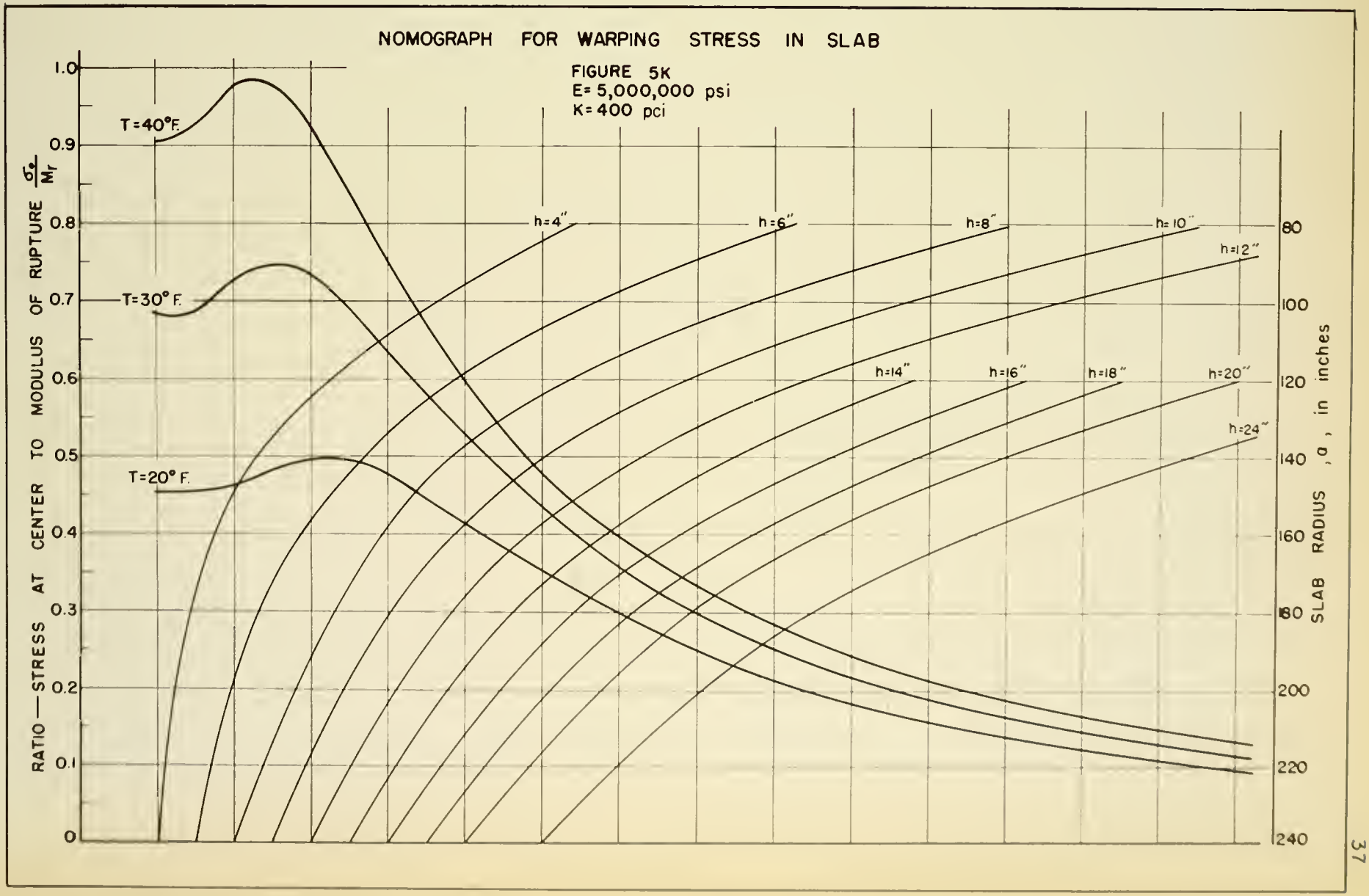
NOMOGRAPH FOR WARPING STRESS IN SLAB
FIGURE 5K
E= 5,000,000 psi
K= 400 pci
RATIO — STRESS AT CENTER TO MODULUS OF RUPTURE σ/Mr
SLAB RADIUS, a, in inches
T=40°F.
T=30°F.
T=20°F.
h=4"
h=6"
h=8"
h=10"
h=12"
h=14"
h=16"
h=18"
h=20"
h=24"
1.0
0.9
0.8
0.7
0.6
0.5
0.4
0.3
0.2
0.1
0
80
100
120
140
160
180
200
220
240

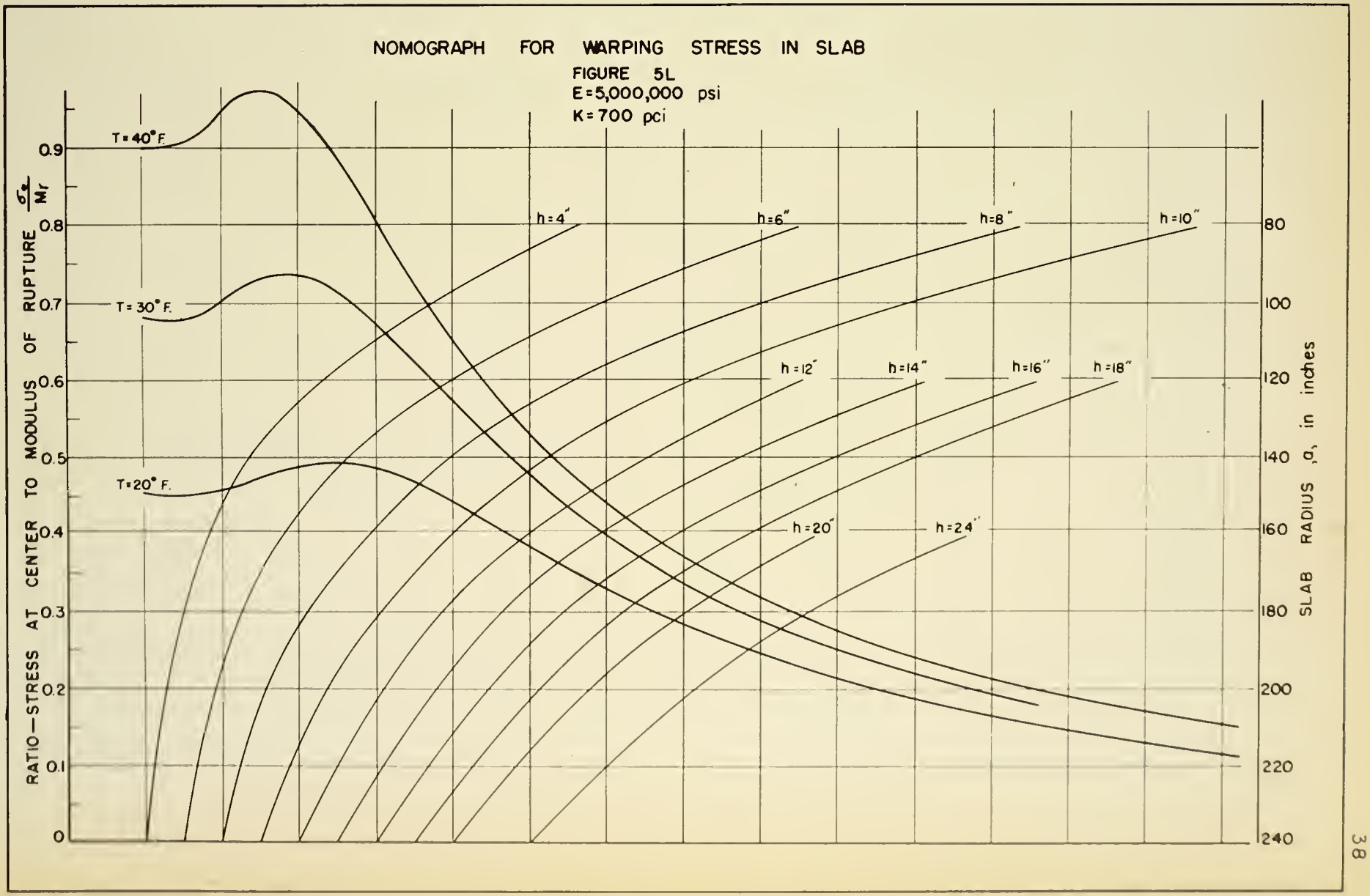
NOMOGRAPH FOR WARPING STRESS IN SLAB
FIGURE 5L
E=5,000,000 psi
K=700 pci
RATIO—STRESS AT CENTER TO MODULUS OF RUPTURE σc/Mr
SLAB RADIUS a, in inches
T=40° F.
T=30° F.
T=20° F.
h=4"
h=6"
h=8"
h=10"
h=12"
h=14"
h=16"
h=18"
h=20"
h=24"
0
0.1
0.2
0.3
0.4
0.5
0.6
0.7
0.8
0.9
80
100
120
140
160
180
200
220
240

RELATIONSHIP BETWEEN MODULUS OF ELASTICITY AND MODULUS OF RUPTURE

FIGURE 6

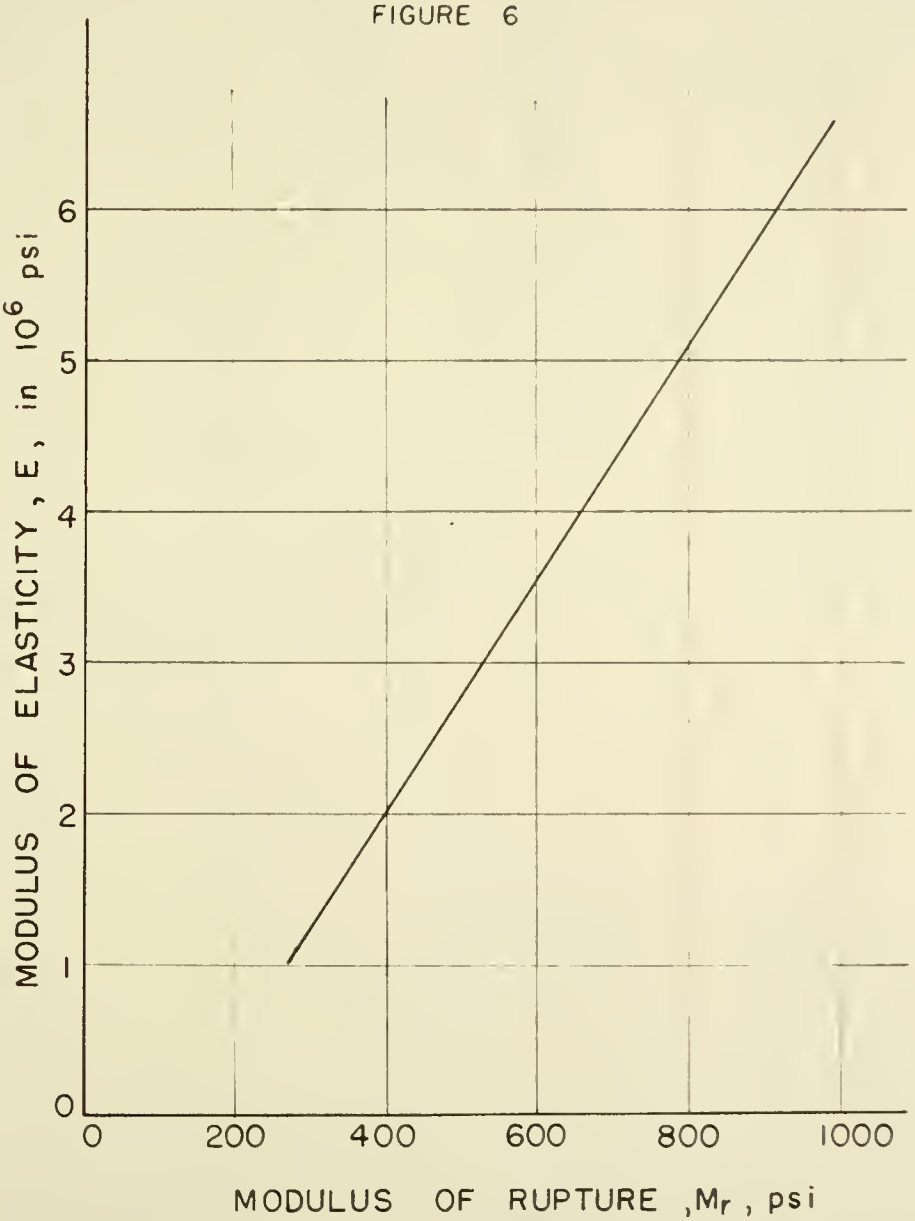


FROM MARIN (27) AND JOINT COMMITTEE ON STANDARD SPECIFICATIONS FOR CONCRETE (21).

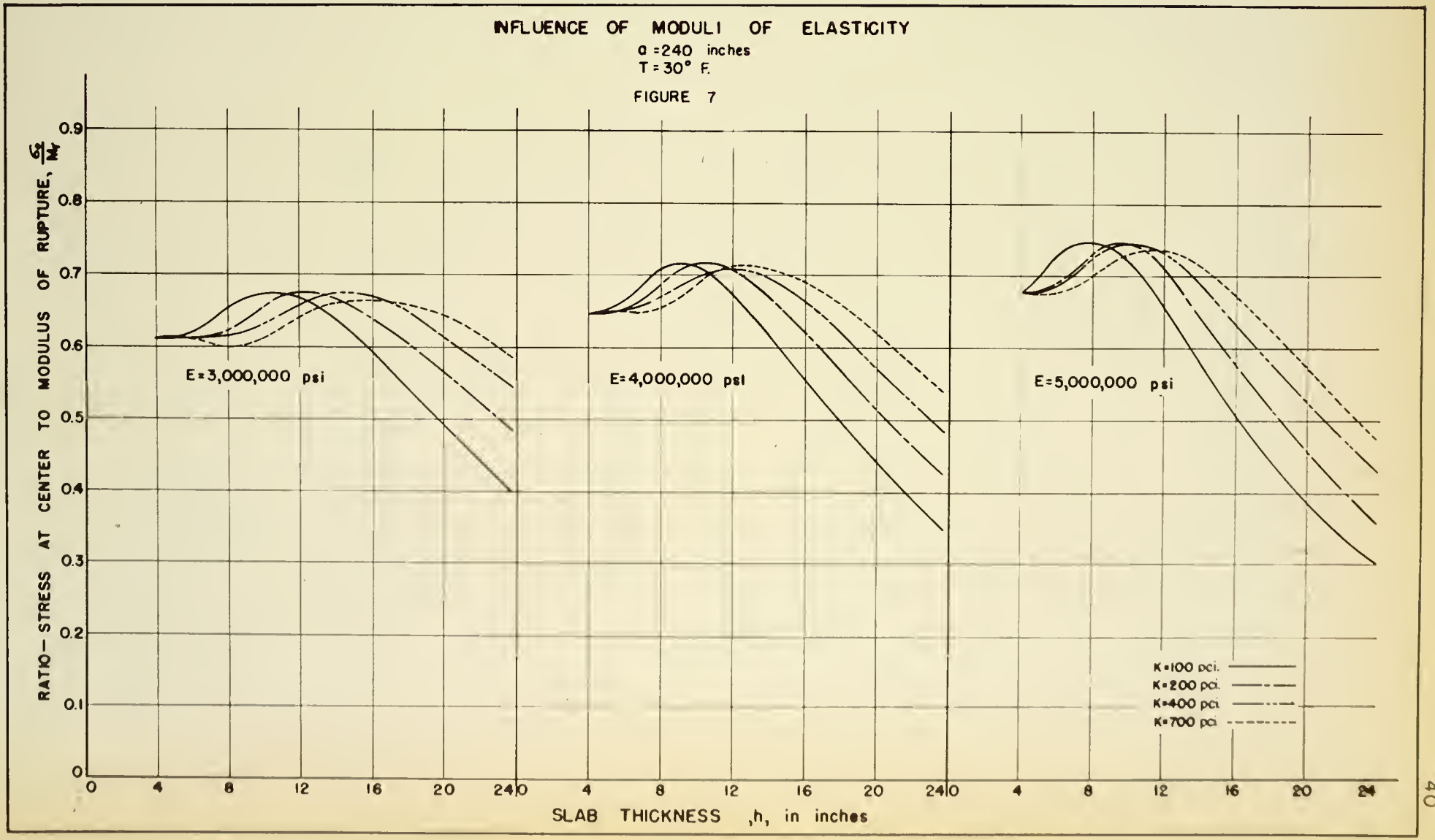
INFLUENCE OF MODULI OF ELASTICITY
a = 240 inches
T = 30° F.
FIGURE 7
RATIO — STRESS AT CENTER TO MODULUS OF RUPTURE, σc/Mr
0.9
0.8
0.7
0.6
0.5
0.4
0.3
0.2
0.1
0
E=3,000,000 psi
E=4,000,000 psi
E=5,000,000 psi
K=100 pci.
K=200 pci.
K=400 pci.
K=700 pci.
0
4
8
12
16
20
24
SLAB THICKNESS ,h, in inches

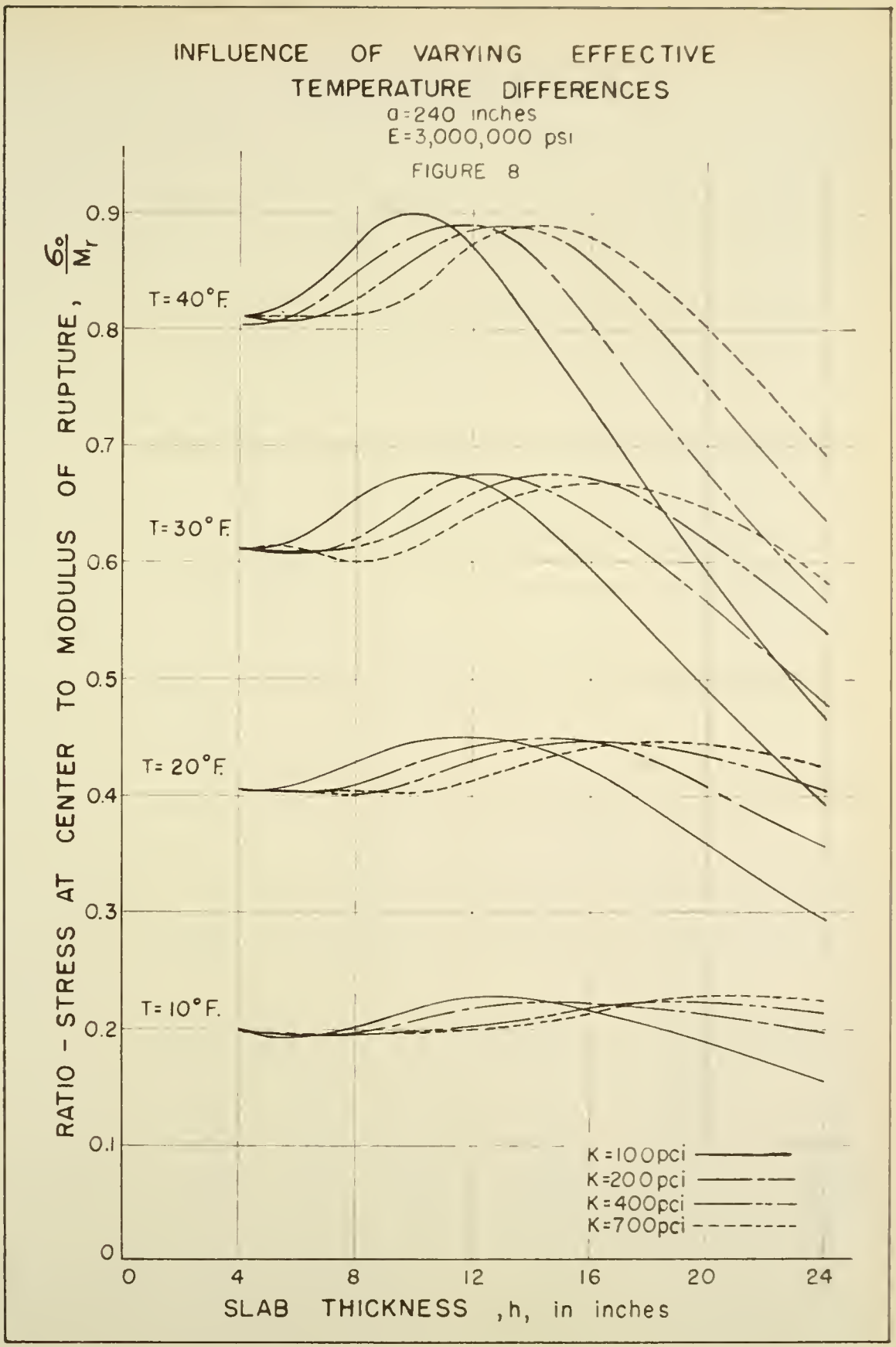
INFLUENCE OF VARYING EFFECTIVE TEMPERATURE DIFFERENCES
a=240 inches
E=3,000,000 psi
FIGURE 8
RATIO - STRESS AT CENTER TO MODULUS OF RUPTURE, $\frac{\sigma_o}{M_r}$
0.9
0.8
0.7
0.6
0.5
0.4
0.3
0.2
0.1
0
T=40°F.
T=30°F.
T=20°F.
T=10°F.
K=100pci
K=200pci
K=400pci
K=700pci
0
4
8
12
16
20
24
SLAB THICKNESS ,h, in inches

# DISCUSSION OF RESULTS

## Examination of Assumptions

In the derivation of the theory it was assumed that the slab had a free edge boundary. This was believed to be justifiable as the only loads considered are those due to the weight of the slab; separate slabs would be subjected to the same effective gradient, thus resulting in little shear or moment transfer. Actual field deflection measurements reported by Hveem (18) appear to substantiate this assumption.

Highway and airport pavement slabs are rectangular in shape rather than circular. The circular shape was selected for study because solutions could be obtained in closed form for finite slab sizes.

Figure 9 represents a plot of the ratios of the normal stress at the center of a circular slab to the normal stress at the center of an infinitely long slab, as given by Westergaard, where the diameter of the circular slab is equal to the width of the long slab. As noted earlier, Westergaard's solution was predicated on the assumption that the subgrade provides full and continuous support to the pavement at all times; hence, the stresses in the circular slabs were computed for full subgrade support. Typical slab diameters corresponding to a $W/\ell$ ratio of 8 are tabulated below:*

| | | | K = 200 pci | | K = 700 pci | |
|---|---|---|---|---|---|---|
| E | μ | h | W=2a | T | W=2a | T |
| $3 \times 10^6$ psi | 0.15 | 8" | 19.0' | 4.36°F | 13.9' | 2.33°F |
| $3 \times 10^6$ psi | 0.15 | 10" | 22.4' | 4.87°F | 16.4' | 2.61°F |
| $3 \times 10^6$ psi | 0.15 | 12" | 25.7' | 5.34°F | 18.8' | 2.85°F |

*See page 59 for list of symbols.

RATIO OF NORMAL STRESS AT CENTER OF CIRCULAR SLAB TO NORMAL STRESS AT CENTER OF INFINITELY LONG STRIP OF FINITE WIDTH* FOR CONDITIONS OF COMPLETE SUPPORT

FIGURE 9

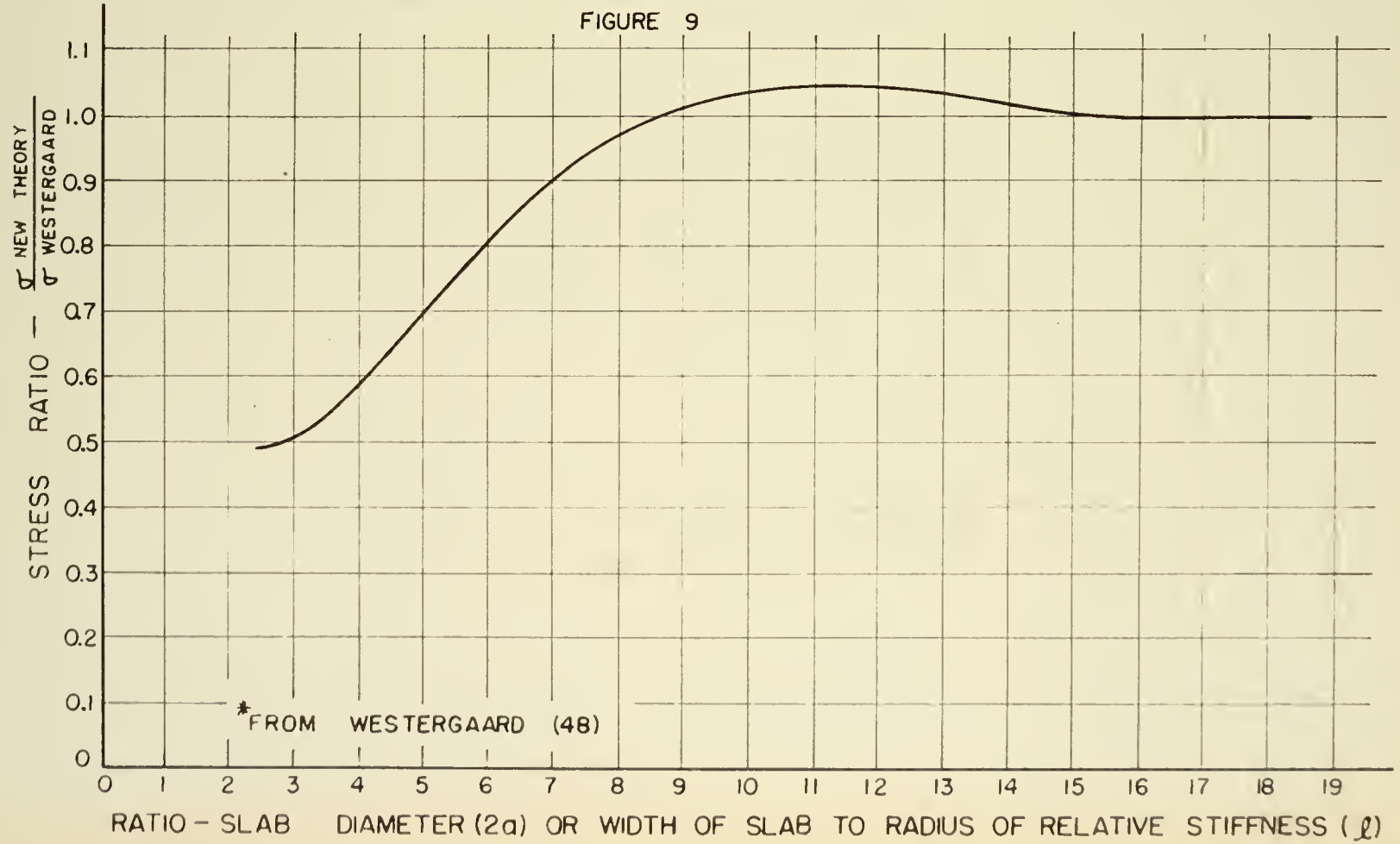

Thus, for slab diameters larger than those corresponding to a $W/\ell$ ratio of 8, the shape of the slab does not appear to be of much importance. The comparisons between computed and measured deflections of warped slabs, to be reported below, lend further weight to the validity of this observation.

Referring to the above tabulation, it is seen that the maximum equivalent temperature difference for which the Westergaard theory is applicable is very much lower than that commonly encountered in practice.

## Comparisons with Available Measurements

Reference was made previously to measured slab deflections obtained by Hatt (page 7). Curves 2 and 4 of Figure 1 are reproduced as solid lines in Figure 10. Curve 2 represents the maximum position of the slab during the drying cycle, whereas curve 4 depicts the maximum position of the slab resulting from drying the slab completely and then introducing water into the subbase and maintaining its level at the lower surface of the slab. The deflection measurements were taken at times when the temperatures were constant throughout the slab. No information was given on the modulus of subgrade reaction of the foundation or on the modulus of elasticity of the concrete. To compare the measured deflections with those computed on the basis of the proposed theory, parameters thought to be equivalent to those of Hatt were chosen.

As the modulus of elasticity of concrete is known to increase both with the duration of wetting and age (45), a modulus of elasticity of 3,500,000 psi was chosen for comparison with curve 4, and 3,000,000 psi for curve 2. The choice of appropriate moduli of subgrade reaction (K) was made on the basis of the moisture condition of the base; thus, a K of 50 pci was used for curve 4 and a K of 150 pci for curve 2.

## COMPARSION BETWEEN OBSERVED AND COMPUTED DEFLECTIONS — HATT

FIGURE 10

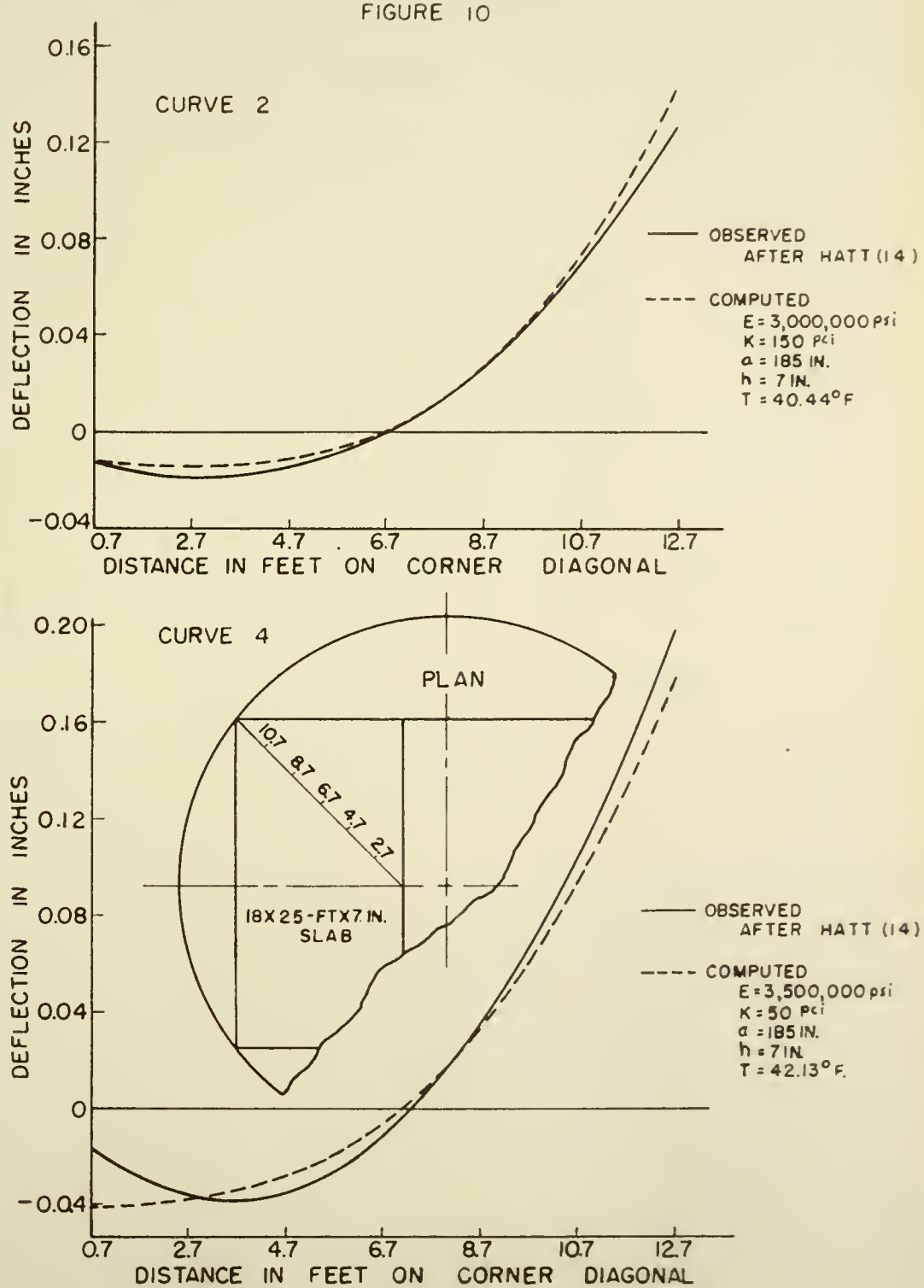

The dotted curves in Figure 10 were obtained by substituting the above parameters into the derived equations. Attention is directed to the computed effective temperature differences (T), shown in Figure 10, which in this case reflect the effects of moisture gradients only.

No comparisons could be made with curve 3 of Figure 1, as the temperature and moisture gradients are zero. According to Hatt, the slight distortion is due to, "----the more pronounced contraction of the richer or troweled surface than of the body of the slab."

The solid curve in Figure 11 represents the longitudinal deflection curve of a rectangular (12 × 24 feet) slab, six inches thick, as measured at the Portland Cement Association Laboratories, Skokie, Illinois. This slab was subject to both temperature and moisture gradients. Comparisons between theoretical and observed deflections for this slab are of special interest, since both the modulus of subgrade reaction (K = 80 pci) of the base and the dynamic modulus of elasticity (4,500,000 psi) of the concrete were determined. Reducing the dynamic modulus of elasticity of concrete to an equivalent static modulus (45), and using an equivalent circular slab 24 feet in diameter, the dotted curve in Figure 11 was obtained.

The correspondence between the computed and measured deflections, as shown in Figures 10 and 11, offers substantial additional evidence regarding the validity of the proposed theory and of the minor importance of the shape of the slab on the critical stresses and deflections.

COMPARSION BETWEEN OBSERVED AND COMPUTED DEFLECTIONS — PORTLAND CEMENT ASSOCIATION

FIGURE 11

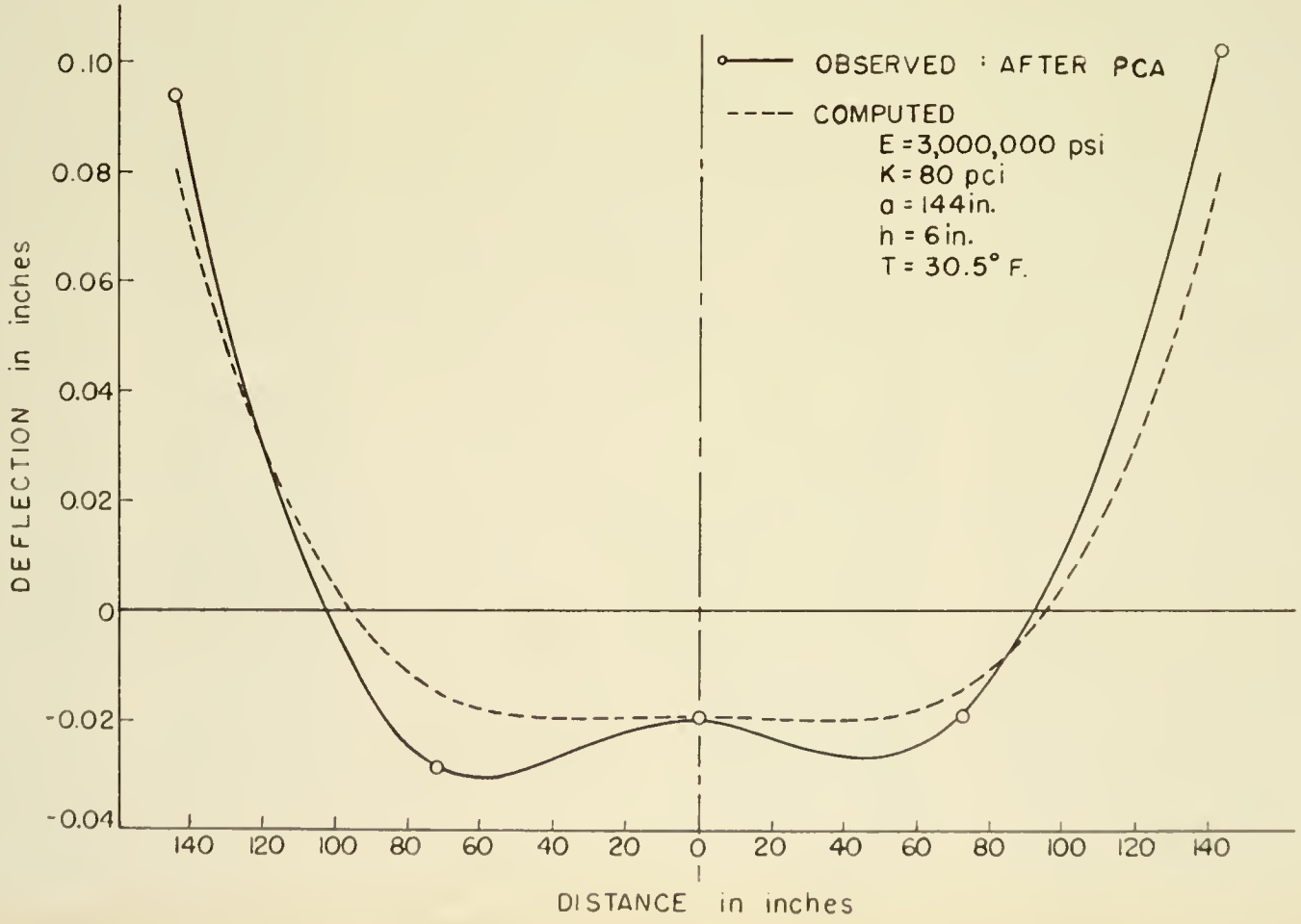

## Effective Gradients

The results of Figures 5A to 5L show that effective temperature differences between slab surfaces of approximately 40 degrees F. are needed to produce tensile stresses which approach the modulus of rupture of the slabs. It has been shown (5, 41) that the temperature gradient in highway pavement slabs is hardly likely to exceed 1-1/2 to 2 degrees F. per inch of slab thickness. Accordingly, critical warping conditions can develop only if appreciable moisture gradients are also present.

As demonstrated by Hatt (14), moisture differences between the top and bottom of slabs result in warping in much the same manner as temperature variations. However, very little is known of these moisture gradients, due to the lack of suitable instrumentation capable of measuring transient moisture gradients in concrete slabs.

Using fragments broken from specimen slabs and determining the moisture content by drying in the laboratory, Teller and Sutherland (41) reported a seasonal variation of moisture content of 0.3 percent. However, they state in their conclusions:

> There is a cyclic variation in slab length that is entirely dissociated from temperature changes. The annual variation in the length of the test sections from causes other than temperature changes is approximately equivalent to that caused by a temperature change of 30°F., and the maximum length occurs during the late winter when the ground moisture content is greatest.

Hveem (18) showed that changes in moisture content for 30 oven-dried thin concrete discs (obtained from pavement cores), which were allowed to soak for 7 days, evidenced a greater percent expansion for 2/3 of the specimens than did a 90°F. increase in temperature. Hveem concluded that,

"In the majority of cases, however, it appears that under road conditions the expansions due to moisture and to temperature would be approximately the same." On the other hand, Shideler (35) and Kalousek (22) have demonstrated that a 2 percent change in moisture in the critical range can account for over 70 percent of the total volume change of concrete masonry units (cf. Figure 12). Thus, large volume changes may be anticipated in highway pavements with but small moisture differences between slab surfaces. Although many factors, such as aggregates, water-cement ratios, curing, carbonation, etc., affect the moisture content-volume change relationship, the available data strongly indicate that combined temperature and moisture gradients encountered in practice are capable of producing tensile stresses which exceed the modulus of rupture of concrete.

It is recognized that permanent distortions of concrete slabs may result from residual differential shrinkage and carbonation (35). However, the available field data previously cited (page 44) indicate that these distortions may be minor in comparison with those produced by temperature and moisture gradients.

## Effects of Warping

The foregoing results show that warping can induce stresses of sufficient magnitude to cause cracking of concrete highway pavements. As the stresses are more critical in the longitudinal direction, transverse cracks in existing pavements can result from this warping, even in the absence of superimposed loads due to traffic. When large segments of the slab are unsupported, more critical stress conditions develop in

SHRINKAGE VS WATER CONTENT
FOR CONCRETE MASONRY UNITS

FIGURE 12

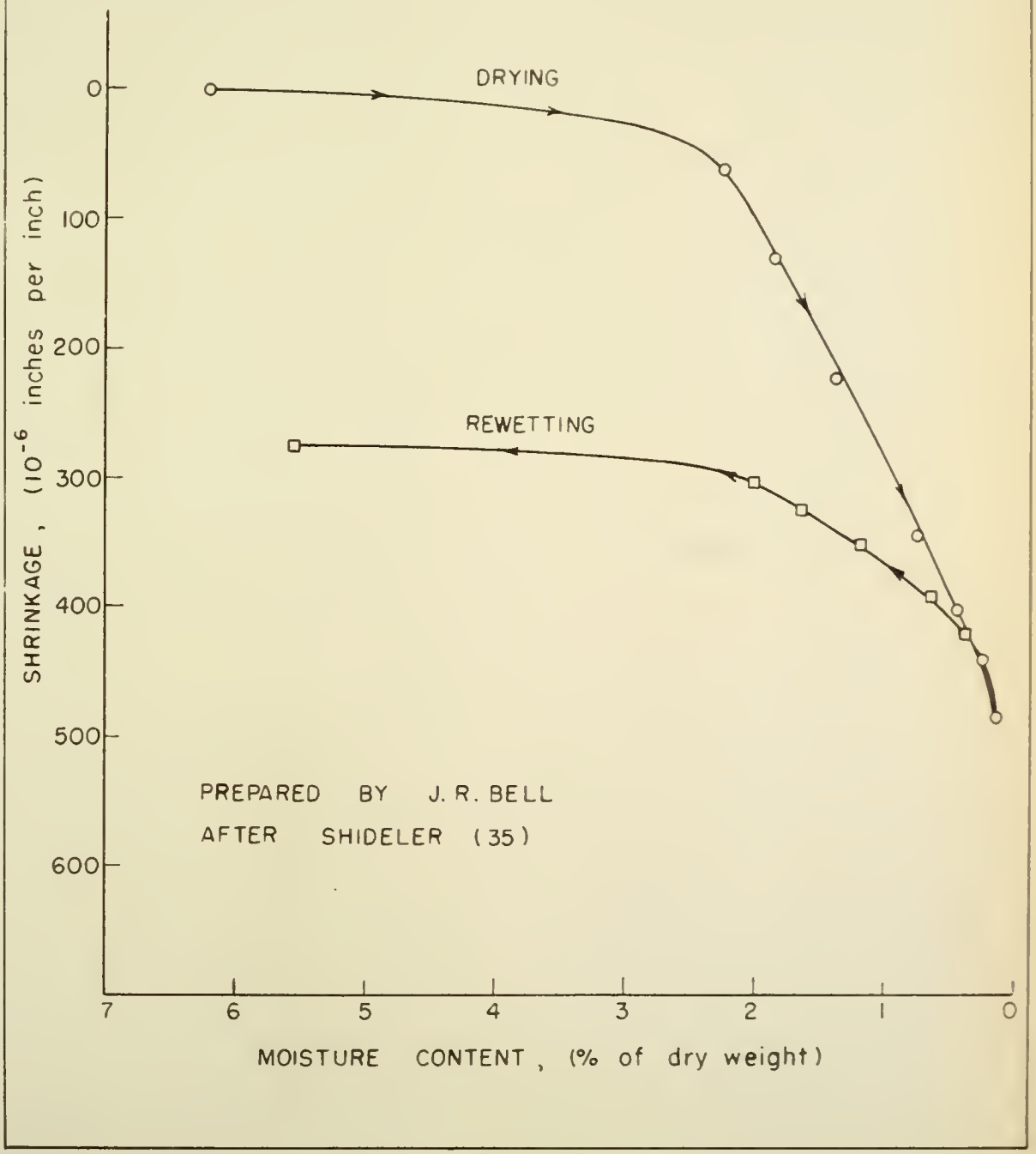

the slab than those which would be computed on the assumption that the slab is fully supported. These facts emphasize the need for more realistic design criteria than are now extant. In addition, warping develops conditions favorable to the entrance of water under the pavement, accelerating the detrimental effects of pavement "pumping."

Warping of pavements is also of importance from the standpoint of the interpretation of deflection and strain measurements induced by external loads. Clearly, the strain and deflection registered at a point in the pavement is greatly influenced by the position of the pavement relative to the subgrade at the time of loading. Even in the few cases where attempts were made to approximate an unstrained and fully supported initial condition in the pavement (by shading the slab from direct sunlight), it is quite probable that warping due to moisture gradients did occur. Accordingly, unless these effects have been properly accounted for, interpretations of pavement performance on the basis of relationships between applied loads and measured strains or deflections should be viewed with caution.

# SUGGESTIONS FOR FURTHER RESEARCH

The results of this study indicate a vital need for a reliable and accurate device to measure transient moisture gradients in hardened concrete slabs.

An intensive search of the literature revealed the paucity of reliable data on the warping of concrete slabs. Thus, conclusive evidence regarding the reliability of warping theories is not available at this time. The value of such a study, under field conditions, can hardly be over-estimated. Advantage could be taken of recent knowledge and advances in instrumentation to determine the absolute position of the pavement and the pavement base at a sufficient number of locations to obtain at any instant the contour of both the slab and its support. These data could be correlated with the prevailing temperature and moisture gradients, permitting valid comparisons between the theory and field performance.

The theory can readily be amplified to investigate the degree of warping and pavement support induced by temperatures and/or moisture contents which decrease with the depth of the slab. Extension of the theory to account for effects of superimposed loads on the warped slab would lead directly to improved design concepts for concrete highway and airport pavements, and to design criteria for "slab on ground" construction for homes.

The development of mix designs that would materially reduce volume changes in the hardened concrete due to moisture and temperature variations, and due to carbonation, would be a major contribution to improved performance of concrete highway and airport pavements.

# CONCLUSIONS

1. On the basis of the assumptions stated herein, a theory has been developed whereby the stresses, deflections, and degree of support of slabs, subject to warping caused by ambient temperature and/or moisture gradients, can be computed for finite slab sizes.

2. Comparisons with available field data strongly indicate that the theory is applicable to concrete pavements not subjected to superimposed loads. Under these circumstances, the following conclusions are justified:

    a. Combined temperature and moisture gradients encountered in practice are capable of producing tensile stresses which exceed the modulus of rupture of concrete highway slabs.

    b. Equivalent temperature gradients at which warped slabs would maintain full contact with their support are very much lower than those normally encountered in practice.

    c. Warping due to temperature and/or moisture gradients develops conditions favorable to the entrance of water under the slab, accelerating the detrimental effects of pavement "pumping." Warping is also a contributing factor to the development of pavement "blowups."

    d. Consideration of the effects of warping is a necessary prerequisite to the interpretation of pavement performance on the basis of measured strains and/or deflections of the slab.

e. In the critical shrinkage range, a moisture gradient of one percent can cause warping equivalent to a 20 degree F. temperature gradient. Accordingly, cracking may occur at small temperature gradients if moisture differences between slab surfaces are only a few percent.

f. A comprehensive investigation of warping in highway pavement slabs, carried out under field conditions with due consideration to defining the initial position and the degree of support, would contribute significantly to the improvement of design concepts.

3. The concepts developed in this study can provide the basis for the solution of a number of problems involving warping of slabs; for example, "slab on ground" construction for homes, icing of lakes, and the like.

# BIBLIOGRAPHY

# BIBLIOGRAPHY


1. Allen, C. W. and Barbee, J. F., "Pavement Performance Surveys," Highway Research Board Proceedings, Vol. 26 (1946).

2. Anderson, F. P., "Investigational Concrete Pavement in Kentucky," Highway Research Board Proceedings, Vol. 20 (1940).

3. Bauschinger, J., "Tests of Different Portland Cements," Mitteilungen Mechanisch-Technisches Laboratorium, Technischen Hochschule, Munich, 1879, (In German).

4. Bone, A. J., Crump, L. W., and Roggeveen, V. J., "Control of Reflection Cracking in Bituminous Resurfacing Over Old Cement Concrete Pavements," Highway Research Board Proceedings, Vol. 33 (1954).

5. Bradbury, R. D., "Reinforced Concrete Pavements," Wire Reinforcement Institute, Washington, D. C., (1938).

6. Breeman, W., "Current Design of Concrete Pavement in New Jersey," Highway Research Board Proceedings, Vol. 28 (1948).

7. Buchanan, S. J., and Khuri, F. I., "Elastic and Plastic Properties of Soils and Their Influence on the Continuous Support of Rigid Pavements," U. S. Army Corps of Engineers, June, 1954.

8. Cashell, H. B., and Teske, W. E., "Continuous Reinforcement in Concrete Pavements," Highway Research Board Proceedings, Vol. 34 (1955)

9. Farrel, F. B., and Patrick, H. R., "The Capital Investment in Highways," Highway Research Board Proceedings, Vol. 32 (1953).

10. Friberg, B. F., "Frictional Resistance Under Concrete Pavements and Restraint Stresses in Long Reinforced Slabs," Highway Research Board Proceedings, Vol. 33 (1954).

11. Friberg, B. F., "Pavement Research, Design, and Prestressed Concrete," Highway Research Board Proceedings, Vol. 34 (1955).

12. Geldmacher, R. C., Anderson, R. L., Dunkin, J. W., Partridge, G. R., Harr, M. E., and Wood, L. E., "Subgrade Support Characteristics, Experimental, Theoretical," Highway Research Board Proceedings, Vol. 36 (1957).

13. Goldbeck, A. T., and Jackson, F. H., "The Expansion and Contraction of Concrete and Concrete Roads," Bulletin No. 532, U. S. Department of Agriculture, (1917).

14. Hatt, W. K., "The Effect of Moisture on Concrete," Transactions of the American Society of Civil Engineers, Vol. 89 (1926).

15. Hetényi, M., "Beams on Elastic Foundation," The University of Michigan Press, Ann Arbor, Michigan, (1946).

16. Highway Research Board Research Reports, No. 3B, "Investigational Concrete Pavements, Progress Reports of Cooperative Research Projects on Joint Spacing," (1945).

17. Highway Research Board Special Report 4, "Road Test One-MD," (1952).

18. Hveem, F. N., "Slab Warping Affects Pavement Joint Performance," Journal of the American Concrete Institute, Vol. 47, pp. 797-808 (1951).

19. Hveem, F. N., "Types and Causes of Failure in Highway Pavements," Preprint of Paper Presented at 37th Annual Meeting of the Highway Research Board, Washington, D. C., January, 1958.

20. Jackson, F. H., and Allen, H., "Concrete Pavements on the German Autobahnen," Journal of the American Concrete Institute, Vol. 44, pp. 933-976 (1948).

21. Joint Committee on Standard Specifications for Concrete and Reinforced Concrete, "Recommended Practice and Standard Specifications for Concrete and Reinforced Concrete," American Concrete Institute, 1947.

22. Kalousek, G. L., O'Heir, R. J., Ziems, K. L., and Saxer, E. L., "Relation of Shrinkage to Moisture Content in Concrete Block," Proceedings of American Concrete Institute, Vol. 50, (1954).

23. Kelly, E. F., "Applications of the Results of Research to the Structural Design of Concrete Pavements," Public Roads, Vol. 20 (1939).

24. Lang, F. C., "Temperature and Moisture Variations in Concrete Pavements," Highway Research Board Proceedings, Vol. 21, (1941).

25. Lang, F. C., "Investigational Concrete Pavement in Minnesota," Highway Research Board Proceedings, Vol. 20, (1940).

26. Lewis, D. W., "The Performance of Concrete Resurfacing in Indiana," Highway Research Board Proceedings, Vol. 30, (1950).

27. Marin, J., "Engineering Materials," Prentice-Hall, Inc., N. Y., (1952).

28. Melan, E., and Parkus, H., "Warmespannungen," Springer-Verlag, Vienna, (1953).

29. Older, C., "Highway Research in Illinois," Proceedings of American Society of Civil Engineers, Vol. 50, pp. 175-217, (1924).

30. Paxson, G. S., "Investigational Concrete Pavement in Oregon, Highway Research Board Proceedings, Vol. 21, (1941).

30a. Phillippe, R. R., and Mellinger, F. M., "Structural Behavior of Heavy-Duty-Concrete Airfield Pavements," Highway Research Board Proceedings, Vol. 31 (1952).

30b. Pickett, G., and Janes, W. C., "Bending Under Lateral Load of a Circular Slab on an Elastic Solid Foundation," Proceedings of the First Midwestern Conference on Solid Mechanics, Urbana, Illinois (1953).

31. Portland Cement Association, "Concrete Pavement Design," Chicago,(1951).

32. Reagel, F. V., "Investigational Concrete Pavement in Missouri," Highway Research Board Proceedings, Vol. 21, (1941).

33. Roberts, S. E., "Cracks in Asphalt Resurfacing Affected By Cracks in Rigid Base," Highway Research Board Proceedings, Vol. 33, (1954).

34. Schleicher, F., "Kreisplatten auf elastischer Unterlage," Julius Springer, Berlin, (1926).

35. Shideler, J. J., "Investigation of the Moisture-Volume Stability of Concrete Masonry Units," Bulletin D3, Portland Cement Association, Chicago, (1955).

35a. Siess, C. P., and Newmark, N. M., "Rational Analysis and Design of Two-Way Concrete Slabs," Proceedings of the American Concrete Institute, Vol. 45 (1949).

36. Spangler, M. G., "Stresses in the Corner Region of Concrete Pavements," Iowa Engineering Experiment Station, Bulletin 157 (1942).

37. Sparkes, F. N., "Stresses in Concrete Road Slabs," Structural Engineer, Vol. 17, Part 2, pp. 98-116, (1939).

38. Sparkes, F. N., and Smith, A. F., "Concrete Roads," Edward Arnold and Company, London, (1952).

39. Stanton, T. E., "Investigational Concrete Pavement in California," Highway Research Report No. 3B, (1945).

40. Sutherland, E. C., discussion to, "Thickness of Concrete Pavements for Highways," by J. H. Moore, Transactions of American Society of Civil Engineers, Vol. 121, (1956).

41. Teller, L. W., and Sutherland, E. C., "The Structural Design of Concrete Pavements," Public Roads, October, 1935; November, 1935; December, 1935; September, 1936; October, 1936; April-May-June, 1943.

42. Terzaghi, K., "Evaluation of Coefficients of Subgrade Reaction," Geotechnique, Vol. V, December, 1955.

43. Thomlinson, J., "Temperature Variations and Consequent Stresses Produced by Daily and Seasonal T mperature Cycles in Concrete Slabs," Concrete and Constructional Engineering, (1940).

44. Timoshenko, S., "Theory of Plates and Shells," McGraw-Hill, New York, (1940).

45. Troxell, G. E., and Davis, H. E., "Composition and Properties of Concrete," McGraw-Hill, New York, (1956).

46. U. S. Department of Commerce, Bureau of Public Roads, "Highway Statistics - 1953," U. S. Government Printing Office, Washington, D. C., (1954).

47. Westergaard, H. M., "Stresses in Concrete Pavements Computed by Theoretical Analysis," Public Roads, April, 1926.

48. Westergaard, H. M., "Analysis of Stresses in Concrete Roads Caused by Variations of Temperature," Public Roads, May 1927.

49. Westergaard, H. M., "What is Known of Stresses," Engineering News-Record, January 7, 1937.

49a. Westergaard, H. M., "New Formulas for Stresses in Concrete Pavements of Airfields," Transactions of American Society of Civil Engineers, Vol. 113 (1948).

50. White, L. V., and Peyton, R. L., "Condition of Concrete Pavement in Kansas as Affected by Coarse Aggregate," Highway Research Board Proceedings, Vol. 25 (1945).

51. Woods, K. B., and Shelburn, T. E., "Pumping of Rigid Pavements in Indiana," Highway Research Board Proceedings, Vol. 23 (1943).

52. Woods, K. B., and Gregg, L. E., "Pavement Performance Related to Soil Texture and Compaction," Highway Research Board Proceedings, Vol. 24, (1944).

53. Woods, K. B., "Influence of Subgrades and Bases on Design of Rigid Pavements," Reprint No. 59, Engineering Experiment Station, Purdue University, July, 1950.

53a. Woods, K. B., Sweet, H. S., and Shelburne, T. E., "Pavement Blowups Correlated with Source of Coarse Aggregate," Highway Research Board Proceedings, Vol. 25 (1945).

54. Yoder, E. J., "Pumping of Highway and Airfield Pavements," Highway Research Board Proceedings, Vol. 36 (1957).

# APPENDIX I

## Nomenclature

Symbols in parentheses represent the dimensions of:

F = force
L = length
t = temperature

$w$ = deflection, positive in the downward direction, (L)

$q$ = distributed load due to weight of slab $(F/L^2)$

$K$ = modulus of subgrade reaction $(F/L^3)$

$p$ = reaction of subgrade, $p = Kw$, $(F/L^2)$

$h$ = slab thickness (L)

$\mu$ = Poisson's ratio

$E$ = Young's modulus

$D = \frac{Eh^3}{12(1-\mu^2)}$ = the flexural rigidity of the slab (FL)

$\ell = \sqrt[4]{D/K}$ = radius of relative stiffness (L)

$\alpha$ = linear coefficient of thermal expansion $(t^{-1})$

$T$ = temperature difference between upper and lower slab surfaces (t)

$r$ = radial distance (L)

$a$ = slab radius (L)

$b$ = radial distance to point of zero deflection (L)

$\beta = \frac{b}{\ell}$

$\rho = \frac{r}{\ell}$

$w'(r)$ = slope at point r

$V(r)$ = shear at point r (F/L)

$M(r)$ = radial bending moment at point r (FL/L)

$\sigma(r)$ = radial normal stress at point r $(FL^{-2})$

$q_0$ = normal stress at center of slab $(FL^{-2})$

$C_j$ = coefficients

$Z_i(\rho)$ = Bessel functions

$Z_i'(\rho)$ = first derivative of $Z_i(\rho)$

$\nabla^2 = (\frac{d^2}{dr^2} + \frac{1}{r}\frac{d}{dr})$

ln = natural logarithm

# APPENDIX II

## General Solution

The general differential equation for the deflection of a thin circular plate resting on an elastic foundation is given (34) as:

$$\nabla^4 w = \frac{q-p}{D} . \tag{1}$$

The solution of equation (1) was obtained by Schleicher (34) in the following form:

$$w = \frac{q}{K} (1 + C_1 Z_1(\rho) + C_2 Z_2(\rho) + C_3 Z_3(\rho) + C_4 Z_4(\rho)). \tag{2}$$

where

$$\begin{aligned} Z_1(\rho) &= \tfrac{1}{2} [J_o(\rho \sqrt{+i}\,) + J_o(\rho \sqrt{-i}\,)] \\ Z_2(\rho) &= -\tfrac{i}{2} [J_o(\rho \sqrt{+i}\,) - J_o(\rho \sqrt{-i}\,)] \\ Z_3(\rho) &= Z_1(\rho) + \tfrac{i}{2} [Y_o(\rho \sqrt{+i}\,) - Y_o(\rho \sqrt{-i}\,)] \\ Z_4(\rho) &= Z_2(\rho) + \tfrac{1}{2} [Y_o(\rho \sqrt{+i}\,) + Y_o(\rho \sqrt{-i}\,)]. \end{aligned} \tag{3}$$

$J_o(\rho)$ and $Y_o(\rho)$ are Bessel functions of the first and second kind, respectively, both of zero order. The Z functions, $Z_1(\rho)$ and $Z_2(\rho)$, which are of particular interest in the present problem are the more common $Ber_o(\rho)$ and $-Bei_o(\rho)$. $Z_3(\rho)$ and $Z_4(\rho)$ are related to the $Kei(\rho)$ and $Ker(\rho)$ functions, respectively.

For the region where the plate is unsupported (Figure 2), equation (1) reduces to

$$\nabla^4 w = \frac{q}{D}. \tag{4}$$

The solution of equation (4), as given by Timoshenko (44), is:

$$w = C_5 + C_6 \ln r + C_7 r^2 + C_8 r^2 \ln r + \frac{q r^4}{64 D} . \tag{5}$$

To obtain the particular solution of interest, the following conditions must be satisfied:

$$
\begin{aligned}
&\text{a) } w_1'(0) = 0 \\
&\text{b) } V_1(0) = 0 \\
&\text{c) } w_1(b) = 0 \\
&\text{d) } V_2(a) = 0 \\
&\text{e) } M_2(a) = 0 \\
&\text{f) } w_2(b) = 0 \\
&\text{g) } w_1'(b) = w_2'(b) \\
&\text{h) } M_1(b) = M_2(b) \\
&\text{i) } V_1(b) = V_2(b).
\end{aligned}
\tag{6}
$$

The subscripts 1 and 2 refer to the supported and unsupported regions of the plate, respectively (see Figure 2).

a) $w_1'(0) = 0.$

$$w_1' = \frac{dw}{dr} = \frac{q}{Kl} \{C_1 Z_1'(\rho) + C_2 Z_2'(\rho) + C_3 Z_3'(\rho) + C_4 Z_4'(\rho)\} .$$

As $\rho$ approaches 0, $Z_1'(\rho)$, $Z_2'(\rho)$, and $Z_3'(\rho)$ approach 0 and $Z_4'(\rho)$ approaches infinity; therefore, $C_4$ must equal 0.

b) $V_1(0) = 0.$

The shear in a thin plate subject to a gradient T/h (28) is

$$V = D \left\{\frac{d}{dr} \left[\nabla^2 w + \alpha(1 + \mu) \frac{T}{h}\right]\right\} . \tag{7}$$

As the gradient is assumed to be independent of the radius, equation (7) reduces to

$$V = D \left\{\frac{d}{dr} \nabla^2 w\right\} \tag{8}$$

and

$$V_1(\rho) = \frac{qD}{K\ell^3}\{C_1Z_2'(\rho) - C_2Z_1'(\rho) + C_3Z_4'(\rho)\} .$$

As $\rho$ approaches 0, $Z_1'(\rho)$ and $Z_2'(\rho)$ approach 0 and $Z_4'(\rho)$ approaches infinity; therefore, $C_3$ must equal 0. Thus, equation (2) reduces to

$$w = \frac{q}{K}\{1 + C_1Z_1(\rho) + C_2Z_2(\rho)\} . \tag{9}$$

c) $w_1(b) = 0.$

$$w_1(\beta) = \frac{q}{K}\{1 + C_1Z_1(\beta) + C_2Z_2(\beta)\} = 0$$

and

$$C_1 = -\frac{1 + C_2Z_2(\beta)}{Z_1(\beta)} . \tag{10}$$

d) $V_2(a) = 0.$

Substituting equation (5) into equation (8) yields

$$V_2(r) = D\{\frac{4C_8}{r} + \frac{qr}{2D}\} ,$$

and for $V_2(a) = 0$,

$$C_8 = -\frac{qa^2}{8D} . \tag{11}$$

e) $M_2(a) = 0.$

The bending moment in a thin plate subject to a gradient T/h (28) is

$$M = D[\frac{d^2w}{dr^2} + \frac{\mu}{r}\frac{dw}{dr} + \alpha(1 + \mu)\frac{T}{h}] ; \tag{12}$$

for M(a) = 0, equation (12) becomes

$$\frac{d^2w}{dr^2} + \frac{\mu}{r}\frac{dw}{dr} + \alpha(1+\mu)\frac{T}{h}\Big|_a = 0.$$

Substituting equations (5) and (11), we have

$$\frac{C_6}{a^2}(\mu-1) + 2C_7(1+\mu) - \frac{qa^2}{8D}(2\mu \ln a + 2\ln a + \mu + 3) + \frac{qa^2}{16D}(3+\mu) + \alpha(1+\mu)\frac{T}{h} = 0;$$

combining, we get

$$\frac{C_6(\mu-1)}{a^2} + 2C_7(1+\mu) - \frac{qa^2}{16D}[4(\mu+1)\ln a + (3+\mu)] + \alpha(1+\mu)\frac{T}{h} = 0. \qquad (13)$$

f) $w_2(b) = 0.$

$$w_2(b) = C_5 + C_6 \ln b + C_7 b^2 + C_8 b^2 \ln b + \frac{qb^4}{64D} = 0.$$

Substituting equation (11) for $C_8$, we get the expression:

$$C_5 + C_6 \ln b + C_7 b^2 - \frac{qa^2b^2 \ln b}{8D} + \frac{qb^4}{64D} = 0. \qquad (14)$$

g) $w_1'(b) = w_2'(b).$

$$w_1'(\beta) = \frac{q}{K\ell}\{C_1Z_1'(\beta) + C_2Z_2'(\beta)\}.$$

$$w_2'(b) = \frac{C_6}{b} + 2C_7 b + 2C_8 b \ln b + C_8 b + \frac{qb^3}{16D}.$$

Substituting equation (11) for $C_8$ and combining, we have

$$\frac{C_6}{b} + 2C_7 b - \frac{qa^2b}{8D}(2\ln b + 1) + \frac{qb^3}{16D} - \frac{q}{K\ell}[C_1Z_1'(\beta) + C_2Z_2'(\beta)] = 0. \qquad (15)$$

h) $M_1(\beta) = M_2(b)$

Substituting equations (5) and (9) into equation (12) and combining,

we get

$$\frac{C_6}{b^2}(\mu-1) + 2C_7(1+\mu) - \frac{qa^2}{8D}[2(1+\mu)\ln b + (3+\mu)] + \frac{qb^2}{16D}(3+\mu)$$

$$- \frac{q}{K\ell^2}\left(C_1\left[Z_2(\beta) - \frac{(1-\mu)Z_1'(\beta)}{\beta}\right] - C_2\left[Z_1(\beta) + \frac{(1-\mu)Z_2'(\beta)}{\beta}\right]\right) = 0. \quad (16)$$

i) $V_1(b) = V_2(b)$.

Substituting equations (5), (9), and (10) into equation (8) and combining, we get

$$C_2 = -\left(\frac{Z_2'(\beta) - Z_1(\beta)[a^2-b^2]\frac{1}{2b\ell}}{Z_2(\beta)\,Z_2'(\beta)+Z_1'(\beta)\,Z_1(\beta)}\right). \quad (17)$$

## Calculation of the Stress Equations

As previously noted, equation (12) expressed the radial bending moment as

$$M(r) = D\left[\frac{d^2w}{dr^2} + \frac{\mu}{r}\frac{dw}{dr} + \alpha(1+\mu)\frac{T}{h}\right].$$

Solving for $\alpha(1+\mu)\frac{T}{h}$ in equation (13) and substituting into equation (12) we obtain

$$\frac{M(r)}{D} = C_6(\mu-1)\left(\frac{1}{r^2} - \frac{1}{a^2}\right) + \frac{qa^2}{4D}(1+\mu)\ln\frac{a}{r} - q\frac{(3+\mu)}{16D}(a^2 - r^2).$$

The radial stress in a thin plate (28) is

$$\sigma_r = \frac{Eh}{2(1-\mu^2)}\left[\frac{M(r)}{D}\right];$$

thus,

$$\sigma_r = \frac{Eh}{2(1-\mu^2)} \left[C_6(\mu-1)\left(\frac{1}{r^2} - \frac{1}{a^2}\right) + \frac{qa^2}{4D}(1+\mu) \ln \frac{a}{r} - \frac{q(3+\mu)}{16D}(a^2-r^2)\right] . \quad (18)$$

Equation (18) is valid for the tensile stress at the upper surface of the slab for $b \leq r \leq a$.

In a similar manner the stress at $0 < r \leq b$ or $0 < \rho \leq \beta$ is found to be

$$\sigma_\rho = \frac{Eh}{2(1-\mu^2)} \left[\frac{q}{K\ell^2}\left[C_1\left[Z_2(\rho) - \frac{(1-\mu)Z_1'(\rho)}{\rho}\right] - C_2\left[Z_1(\rho) + \frac{(1-\mu)Z_2'(\rho)}{\rho}\right]\right]\right.$$

$$\left. + \alpha(1+\mu)\frac{T}{h}\right] . \quad (19)$$

At $\rho = 0$, equation (19) reduces to

$$\sigma_o = \frac{Eh}{2(1-\mu^2)} \left[-\frac{C_2 q}{2K\ell^2}(1+\mu) + \alpha(1+\mu)\frac{T}{h}\right] . \quad (20)$$

# APPENDIX III

# TYPICAL CALCULATIONS AS COMPUTED BY HAND CALCULATOR

| | | | | | |
|---|---|---|---|---|---|
| $a$ | 240 | $z_1(\beta)$ | -6.6492 | $E$ | $3 \times 10^6$ |
| $\beta$ | 6.70 | $z_2(\beta)$ | 16 5384 | $\mu$ | 0 15 |
| $b$ | 190 5849 | $z_1'(\beta)$ | 7 5442 | $q$ | 2/3 |
| $l$ | 28.4455 | $z_2'(\beta)$ | 15 1463 | $h$ | 8 |
| $k$ | 200 | | | $a^2$ | 57,600 |
| | | | | $b^2$ | 36,322.5851 |

$$C_2 = -\left\{ \frac{z_2'(\beta) - \frac{z_1(\beta)}{2bl}\left[a^2 - b^2\right]}{z_2(\beta)z_2'(\beta) + z_1'(\beta)z_1(\beta)} \right\}$$

$$C_2 = -\left\{ \frac{(\ 15.1463\ ) - \frac{(-6\ 6492\ )(21277.4149)}{2(190.5849)(28.4455\ )}}{(16.5384\ )(15.1463\ ) + (\ 7.5442\ )(-6\ 6492)} \right\}$$

$$C_2 = -\left\{ \frac{(\ 15.1463\ ) - (-13.0483\ \ \ )}{(\ 250.4954\ ) + (-50.1626\ \ \ )} \right\}$$

$$C_2 = -\ 0.14073$$

$$C_1 = -\frac{1 + C_2 z_2(\beta)}{z_1(\beta)} = -\left\{ \frac{1 + (-0.1407\ )(16.5384\ )}{(\ -6.6492\ \ )} \right\}$$

$$C_1 = -\left\{ \frac{-1.3275}{-6.6492} \right\}$$

$$C_1 = -\ 0.1996$$

$$F_1 = \frac{F}{q} \; ; \quad F = q\left[\frac{1}{K\ell^2}\left\{C_1\gamma - C_2\delta\right\} + \underbrace{\frac{a^2}{8D}\left[(3+\mu)+2(\ln b)(1+\mu)\right] - \frac{b^2}{16D}(3-\mu)}_{G}\right]$$

---

$$\gamma = Z_2(\beta) - \frac{(1-\mu)Z_2'(\beta)}{\beta} = (16.5384) - \frac{(0.85)(75442)}{(6.70)}$$

$$= (16.5384) - (0.9571) = \underline{15.5813}$$

$$\delta = Z_1(\beta) + \frac{(1-\mu)Z_2'(\beta)}{\beta} = (-6.6492) + \frac{(0.85)(151463)}{(6.70)}$$

$$= (-6.6492) + (1.9215) = \underline{-4.7277}$$

$$C_1\gamma = (-0.1995)(15.5813) = \underline{-3.1084}$$

$$C_2\delta = (-0.1407)(-4.7277) = \underline{0.6652}$$

$$C_1\gamma - C_2\delta = \underline{-3.7736}$$

$$\frac{1}{K\ell^2} = \underline{6.1794 \times 10^{-6}}; \quad (C_1\gamma - C_2\delta)\left(\frac{1}{K\ell^2}\right) = \underline{-2.3318 \times 10^{-5}}$$

$$G = \frac{a^2}{8D}\left[(3+\mu)+2(1+\mu)\ln_e b\right] - \frac{b^2}{160}(3+\mu)$$

$$\ln b = \underline{5.25}$$

$$b^2 = \underline{36322.5859}$$

$$G = (5.4984 \times 10^5)\left[(3.15)+(2.3)(5.25)\right] - \frac{(36322.5859)}{(2095.140840)}(3.15) = \underline{78.2522 \times 10^{-5}}$$

$$F_1 = \left\{\left[(C_1\gamma - C_2\delta)\frac{1}{K\ell^2}\right] - G\right\} = \underline{-2.3318 \times 10^{-5} + 78.2522 \times 10^{-5}}$$

$$F_1 = \underline{75.9204}$$

$$C' = \frac{C}{q} \qquad C' = \left[\frac{1}{K\ell}\left\{C_1 Z_1'(\beta) + C_2 Z_2'(\beta)\right\} + J\right]$$

$$J = \frac{a^2 b}{8D}(2 \ln b + 1) - \frac{b^3}{16D}$$

$$C' = \left[(1.7578 \times 10^{-4})\left\{(-0.1996)(7.5442) + (-0.1407)(15.1463)\right\} + J\right]$$

$$C' = \left[(1.7578 \times 10^{-4})\left\{-3.6369\right\} + J\right]$$

$$J = \begin{cases} \dfrac{a^2 b}{8D} = 1047.9177 \times 10^{-5} \\ (2 \ln b \quad 1) = 11.5 \\ \dfrac{a\,b}{8D}(2 \ln b + 1) = 12051.0535 \times 10^{-5} \\ -\dfrac{b^3}{16\,D} = 330.4075 \times 10^{-5} \end{cases}$$

$$J = 1172.0645 \times 10^{-5}$$

$$C' = \left[(-6.3929 \times 10^{-4}) + (1172.0645 \times 10^{-4})\right]$$

$$C' = 1165.6717 \times 10^{-4}$$

$$\frac{C_7}{q} = \frac{F_1 b + (1-\mu)C'}{4b} = 3.1977 \times 10^{-4}$$

$$\frac{C_6}{q} = \frac{b}{2}\left[C'(1+\mu) - F_1 b\right] = -101389.2609 \times 10^{-5}$$

$$\left(\frac{C_6}{q}\right)\left(\frac{\mu-1}{a^2}\right) + \left(\frac{C_7}{q}\right)\left[2(1+\mu)\right] \underbrace{- \frac{a^2}{16D}\left[4(\ln a)(\mu+1) + (\mu+3)\right]}_{H} = \frac{Mt}{Dq}$$

$$H = 7.79703 \times 10^{-4}$$

$$-\frac{Mt}{Dq} = \left[1.4962 \times 10^{-5}\right] + \left[73.5471 \times 10^{-5}\right] - \left[77.9703 \times 10^{-5}\right]$$

$$-\frac{Mt}{Dq} = -2.9270 \times 10^{-5}$$

$$t = \left(\frac{Mt}{Dq}\right)\frac{qh}{(1+\mu)\alpha} = 22.6240$$

# APPENDIX IV

FLOW DIAGRAM OF MAIN PROGRAM
FIGURE 13

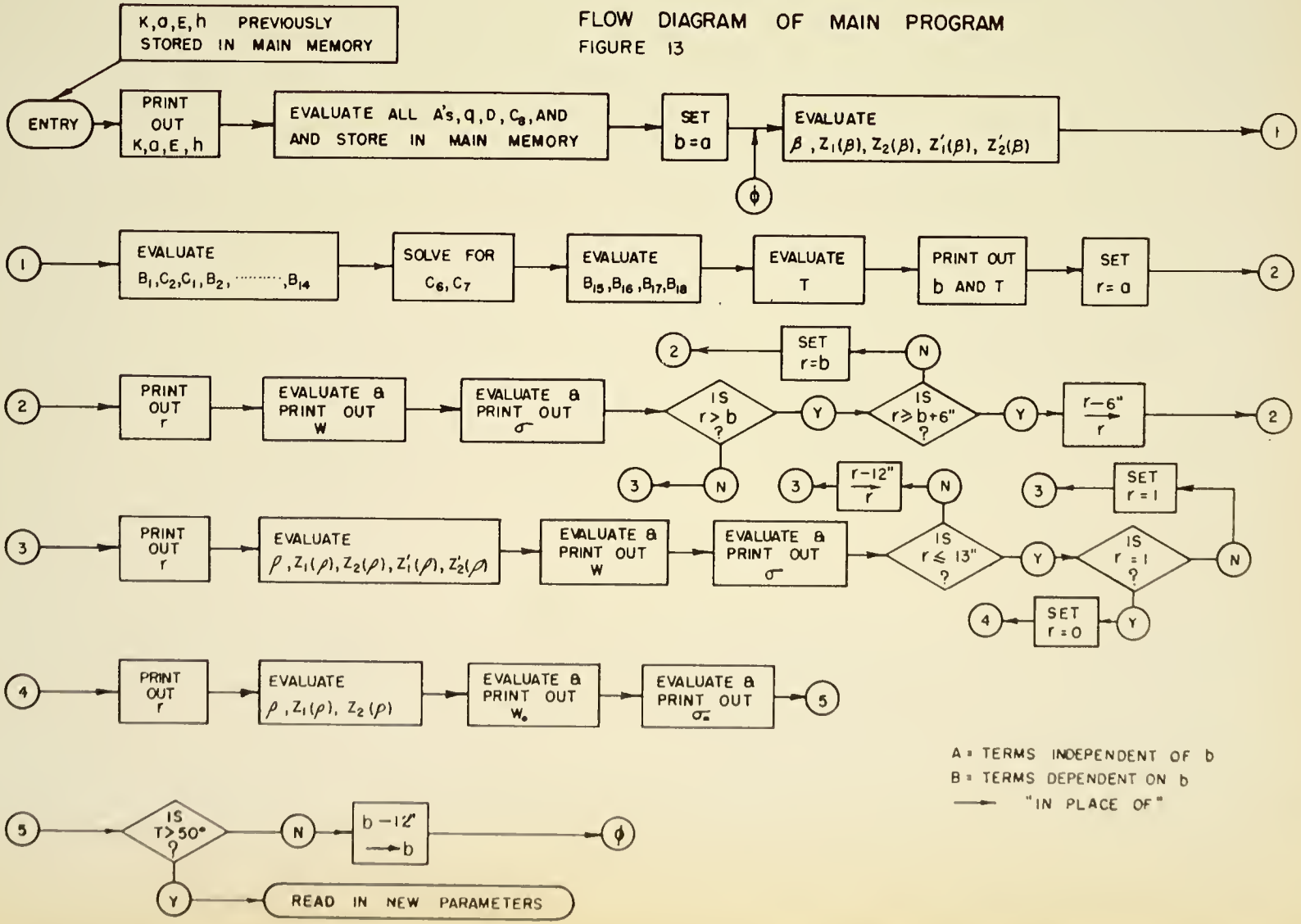

# APPENDIX V

FLOW DIAGRAM OF Ber X

FIGURE 14 A

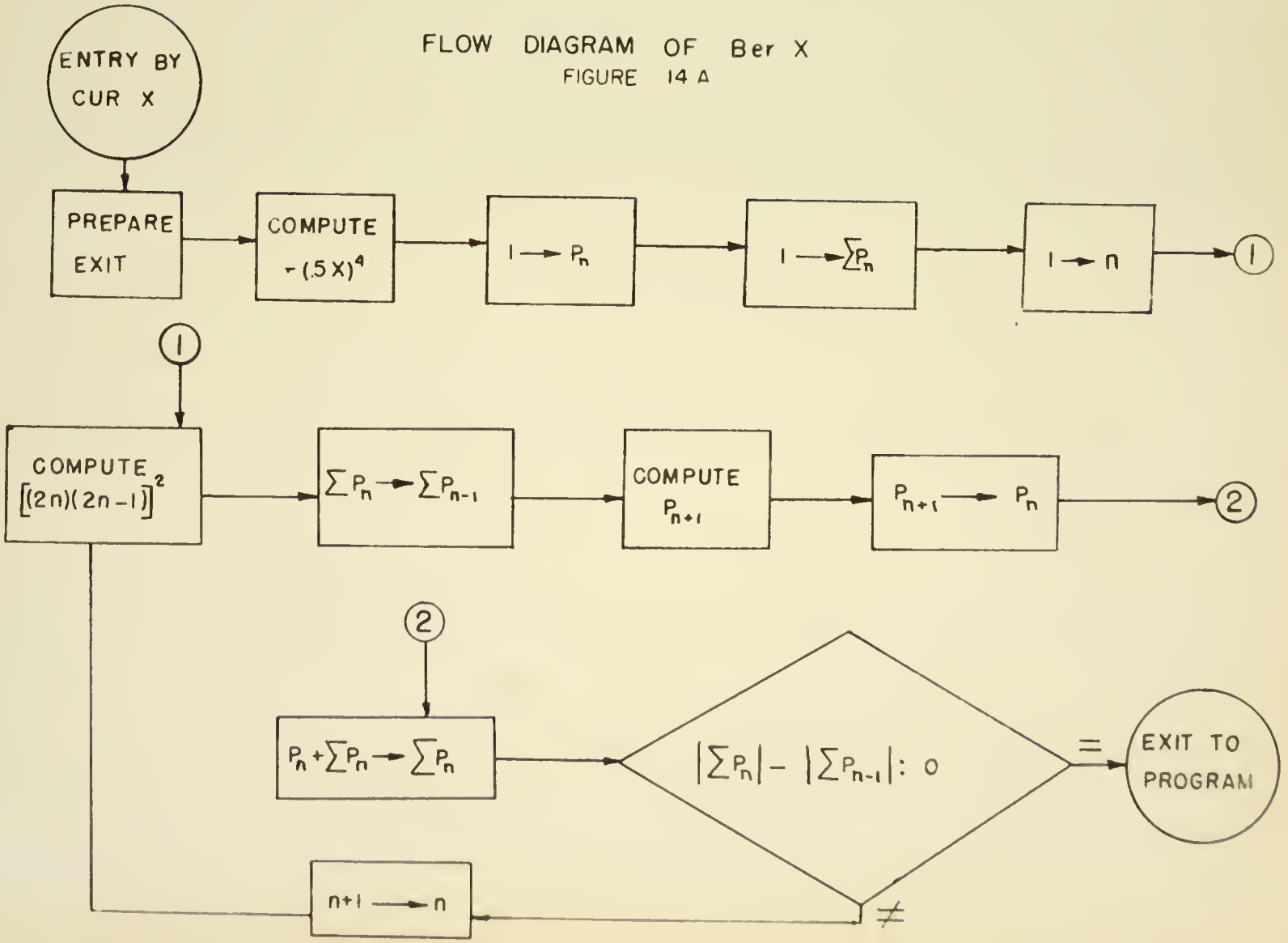

FLOW DIAGRAM OF Bei X

FIGURE 14 B

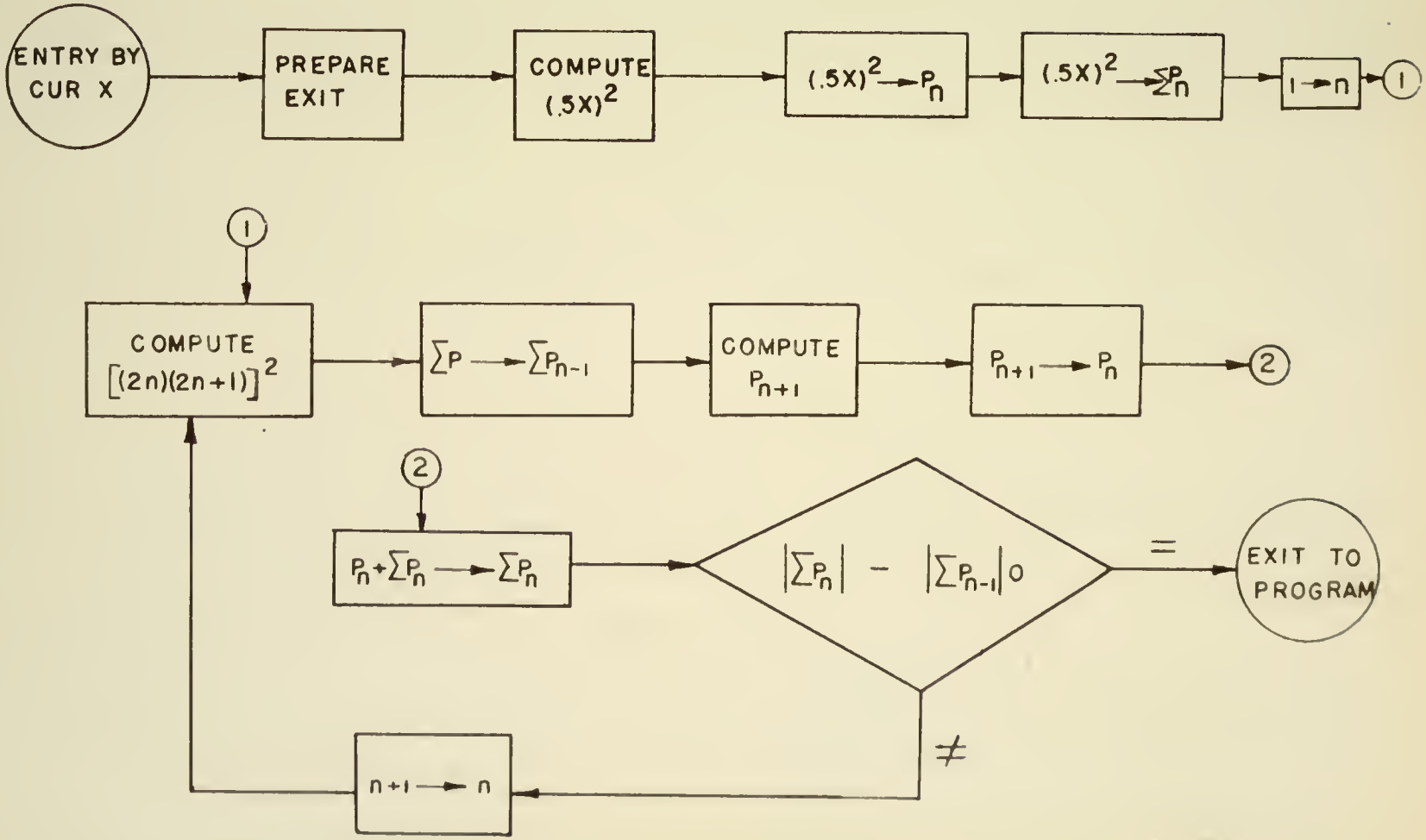

FLOW DIAGRAM OF Ber' X

FIGURE 14 C

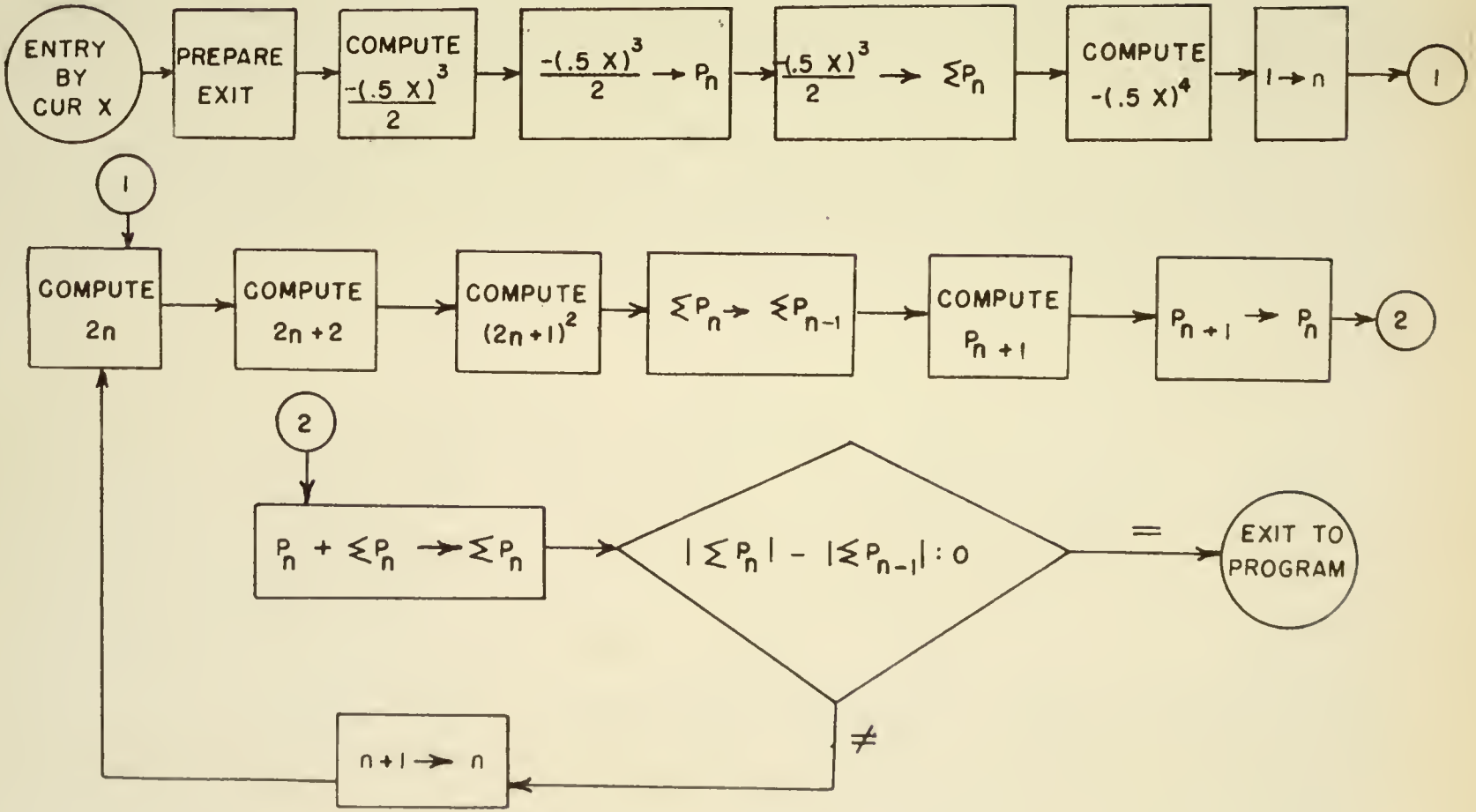

FLOW DIAGRAM OF Bei' X

FIGURE 14 D

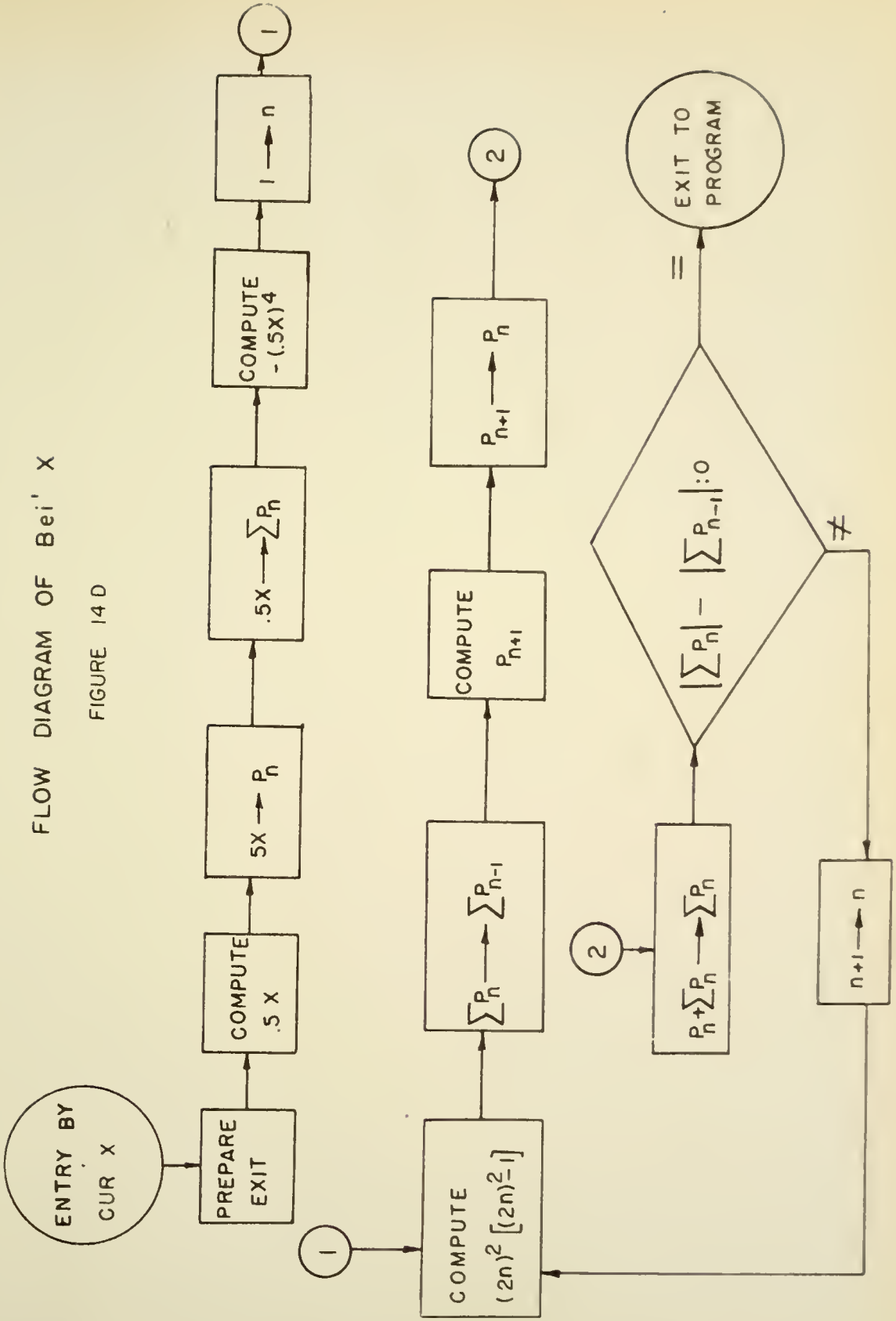

# VITA

# VITA

Milton Edward Harr was born October 19, 1925, at Chelsea, Massachusetts, and received his early education in the Chelsea School System.

In June, 1943, after graduation from Chelsea High School, he enlisted in the United States Navy. After participating in the Normandy Invasion, Mr. Harr was transferred to the United States Marine Corps. He served with the Third Marine Division on Guam and Iwo Jima. Mr. Harr has received the Order of the Purple Heart, the Presidential Unit Citation, and the Navy Unit Commendation.

Upon separation from the service in August of 1945, he entered Northeastern University, receiving his B.S. in Civil Engineering in June, 1949. During the summer of 1948, he was employed as an Assistant Resident Engineer by the Massachusetts Department of Public Works, Highway Division. Upon graduation, he went to work for the Bureau of Reclamation in Provo, Utah. In September, 1949, he returned to the Massachusetts Department of Public Works, where he participated in the design and construction of several major highways.

In 1953, he resigned his position and joined the staff of Rutgers University, receiving his M.S.C.E. in June, 1955. Upon graduation, he went to work for Howard, Needles, Tammen, and Bergendoff as Area Engineer on the widening of the New Jersey Turnpike. He resigned his position in September, 1955, to join the staff of Purdue University as an Instructor in Civil Engineering.

Mr. Harr is a member of Sigma Xi and Chi Epsilon. He is married and has three children.